

Non-Markovian dynamical heat engines

Fabio Cavaliere,^{1,2} Matteo Carrega,² Giulio De Filippis,^{3,4}
Vittorio Cataudella,³ Giuliano Benenti,^{5,6,7} and Maura Sasseti^{1,2}

¹*Dipartimento di Fisica, Università di Genova, Via Dodecaneso 33, 16146 Genova, Italy*

²*CNR-SPIN, Via Dodecaneso 33, 16146 Genova, Italy**

³*SPIN-CNR and Dip. di Fisica “E. Pancini” - Università di Napoli “Federico II” - I-80126 Napoli, Italy.*

⁴*INFN, Sezione di Napoli, Complesso Universitario di Monte S. Angelo, I-80126 Napoli, Italy*

⁵*Center for Nonlinear and Complex Systems, Dipartimento di Scienza e Alta Tecnologia,
Università degli Studi dell’Insubria, via Valleggio 11, 22100 Como, Italy*

⁶*Istituto Nazionale di Fisica Nucleare, Sezione di Milano, via Celoria 16, 20133 Milano, Italy*

⁷*NEST, Istituto Nanoscienze-CNR, I-56126 Pisa, Italy*

(Dated: May 4, 2022)

We discuss whether, and under which conditions, it is possible to realize a heat engine simply by dynamically modulating the couplings between the quantum working medium and thermal reservoirs. For that purpose, we consider the paradigmatic model of a quantum harmonic oscillator, exposed to a minimal modulation, that is, a monochromatic driving of the coupling to only one of the thermal baths. We show that in this setup non-Markovianity of the bath is a necessary condition to obtain a heat engine. In addition, we identify suitable structured environments for the engine to approach the ideal Carnot efficiency. Our results open up new possibilities for the use of non-Markovian open quantum systems for the construction and optimization of quantum thermal machines.

Introduction.— The trend toward miniaturization is pushing heat engines up to the level where the working medium is a small system, which requires quantum mechanics for an accurate description [1–12]. This opened several fundamental and applicative issues in the growing field of quantum thermodynamics [13–26] in the last years. As for any other quantum machine, the interaction of the quantum system with the external world requires special care [2, 4, 12, 23, 24, 27–29]. On one hand, it would be desirable to maintain the system isolated from the environment, to preserve any quantum advantage [5, 30–37] provided by coherent dynamics. On the other hand, a thermal engine delivering finite power requires that work is extracted and heat is exchanged with reservoirs at finite rates. A rigorous treatment of energy exchanges and heat flows is thus required to properly model quantum thermal machines working out of equilibrium. For instance, the coupling, possibly strong, between quantum working medium and baths, can quite naturally induce non-Markovian effects, with backflow of information and energy from baths to working medium [25, 38–46], whose effects are often discarded in conventional approximation schemes [2–4, 15, 22, 41, 47, 48]. The question then arises, whether non-Markovian dynamics may constitute a useful thermodynamic resource.

In this Letter, we address this question for a minimal disturbance of the quantum system, that is, a monochromatic modulation of the coupling to one thermal bath. The same achievement of a heat engine in such a setup, without directly driving the system, is challenging. Indeed, modulation of the couplings is intuitively associated with dissipation, akin to friction induced by moving parts in strokes of a macroscopic heat engine. Non-

Markovianity, which is a feature beyond standard master equation approaches, is here investigated in the paradigmatic model of a quantum harmonic oscillator (QHO), coupled to two bosonic thermal (hot and cold) baths. Such approach is quite versatile, since it is possible to study the QHO dynamics and thermodynamics, without resorting to approximations, both in the quantum and in the classical regime, and for arbitrary spectral features of the environment.

We show that, as counterintuitive as it might seem, a heat engine can be obtained in the above configuration. To achieve such a result, non-Markovianity is a necessary but not sufficient condition. Furthermore, we show that by taking advantage of a suitable structured environment, the engine can even approach the Carnot efficiency.

Model.— The working medium under study is a QHO whose Hamiltonian reads ($\hbar = k_B = 1$) $H_{\text{QHO}} = \frac{p^2}{2m} + \frac{1}{2}m\omega_0^2x^2$, where m and ω_0 are the mass and the characteristic frequency, respectively. The QHO is linearly coupled to two reservoirs, with the total Hamiltonian $H^{(t)} = H_{\text{QHO}} + \sum_{\nu=1}^2 (H_{\nu} + H_{\text{int},\nu}^{(t)})$. Each bath ($\nu = 1, 2$) is modelled as an ensemble of harmonic oscillators in the usual Caldeira-Leggett [27–29, 49, 50] framework with $H_{\nu} = \sum_{k=1}^{\infty} \left(\frac{P_{k,\nu}^2}{2m_{k,\nu}} + \frac{m_{k,\nu}\omega_{k,\nu}^2 X_{k,\nu}^2}{2} \right)$. We assume that the system/baths couplings can be varied in time [24, 42, 51], described by the interaction contribution $H_{\text{int},\nu}^{(t)} = \sum_{k=1}^{\infty} \left\{ -xg_{\nu}(t)c_{k,\nu}X_{k,\nu} + x^2g_{\nu}^2(t)\frac{c_{k,\nu}^2}{2m_{k,\nu}\omega_{k,\nu}^2} \right\}$. The interaction strengths are described by the parameter $c_{k,\nu}$, and the time-dependence of the couplings is in the dimensionless functions $g_{\nu}(t)$. We consider the minimum modulation needed for the couplings in the search for a heat

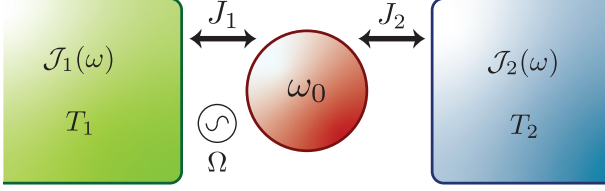


FIG. 1. Sketch of the setup: J_ν represents the energy current flowing between the QHO and the ν -th contact. The two reservoirs are in equilibrium at a temperature T_ν and described by a spectral density $\mathcal{J}_\nu(\omega)$ with $\nu = 1, 2$.

engine, that is, a monochromatic driving for the first contact, $g_1(t) = \cos(\Omega t)$, while the second is kept constant, $g_2(t) = 1$ (see the sketch in Fig. 1). To model bath properties we introduce the bath spectral density as [28]

$$\mathcal{J}_\nu(\omega) = \frac{\pi}{2} \sum_{k=1}^{\infty} \frac{c_{k,\nu}^2}{m_{k,\nu} \omega_{k,\nu}} \delta(\omega - \omega_{k,\nu}), \quad (1)$$

whose precise forms will be specified later. The non-equilibrium dynamic of the QHO obeys the generalized quantum Langevin equation [42, 52, 53]

$$\begin{aligned} \ddot{x}(t) + \omega_0^2 x(t) + \int_{t_0}^{+\infty} ds \sum_{\nu=1}^2 g_\nu(t) \gamma_\nu(t-s) \\ \times \left[\dot{g}_\nu(s) x(s) + \dot{x}(s) g_\nu(s) \right] = \frac{1}{m} \sum_{\nu=1}^2 g_\nu(t) \xi_\nu(t), \quad (2) \end{aligned}$$

where the damping kernels are linked to the spectral func-

$$\begin{aligned} P = \frac{\Omega}{4\pi m} \sum_{\mu=-\infty}^{+\infty} \int_{-\infty}^{+\infty} d\omega \left\{ \frac{\mathcal{J}_2(\omega)}{2m} \coth\left(\frac{\omega}{2T_2}\right) \left| \tilde{G}_\mu(\omega) \right|^2 \left[\mathcal{J}_1(\omega + (\mu + 1)\Omega) - \mathcal{J}_1(\omega + (\mu - 1)\Omega) \right] \right. \\ \left. + \mathcal{J}_1(\omega) \coth\left(\frac{\omega}{2T_1}\right) \left\{ \frac{\mathcal{J}_1(\omega - \mu\Omega)}{4m} \left| \tilde{G}_\mu(-\omega + \Omega) \right|^2 + \tilde{G}_{\mu+2}(-\omega - \Omega) \right|^2 - \text{Im} \left[\tilde{G}_0(\omega - \Omega) \right] \delta_{\mu,0} \right\} \right\}. \quad (6) \end{aligned}$$

Here, we have introduced the Floquet coefficients that satisfy the following algebraic set of equations

$$\begin{aligned} \tilde{G}_\mu(\omega) = \chi(\omega) \delta_{\mu,0} - \chi(\omega + \mu\Omega) \\ \times \sum_{n=\pm 2} \tilde{k}_n(\omega + (\mu - n)\Omega) \tilde{G}_{\mu-n}(\omega), \quad (7) \end{aligned}$$

where $\chi(\omega) = -\left[\omega^2 - \omega_0^2 - \tilde{k}_0(\omega)\right]^{-1}$ and the influence

tion by

$$\gamma_\nu(t) = \frac{2}{\pi m} \theta(t) \int_0^\infty d\omega \frac{\mathcal{J}_\nu(\omega)}{\omega} \cos(\omega t), \quad (3)$$

with $\theta(t)$ the Heaviside step function. We recall that $\xi_\nu(t)$ represents the fluctuating force operator with null quantum average $\langle \xi_\nu(t) \rangle \equiv \text{Tr}[\xi_\nu(t) \rho(t_0)] = 0$ and time correlator $\langle \xi_\nu(t) \xi_{\nu'}(t') \rangle = \delta_{\nu,\nu'} \mathcal{L}_\nu(t - t')$, with

$$\mathcal{L}_\nu(t) = \int_0^\infty \frac{d\omega}{\pi} \mathcal{J}_\nu(\omega) \left[\coth\left(\frac{\omega}{2T_\nu}\right) \cos(\omega t) - i \sin(\omega t) \right]. \quad (4)$$

Note that at initial time $t_0 \rightarrow -\infty$ the baths are assumed in their thermal equilibrium at temperatures T_ν , with the total density matrix, written in a factorized form $\rho(t_0) = \rho_{\text{QHO}}(t_0) \otimes \rho_1(t_0) \otimes \rho_2(t_0)$, where $\rho_{\text{QHO}}(t_0)$ is the initial system density matrix.

We focus on thermodynamic quantities in the long time limit, when a periodic steady state has been reached [54]. The monochromatic drive $g_1(t)$ injects power, whose amount once averaged over one period ($\mathcal{T} = 2\pi/\Omega$) of the driving is given by

$$P = \int_t^{t+\mathcal{T}} \frac{dt'}{\mathcal{T}} \text{Tr} \left[\frac{\partial H_{\text{int},1}(t')}{\partial t'} \rho(t') \right]. \quad (5)$$

At periodic steady state, the averaged injected power is balanced by the reservoir heat currents $J_\nu = -\int_t^{t+\mathcal{T}} \frac{dt'}{\mathcal{T}} \text{Tr}[H_\nu \dot{\rho}(t')]$. That is, $P + \sum_{\nu=1}^2 J_\nu = 0$ (for a proof of this equality, see [54]), which can be interpreted as a manifestation of the first law of thermodynamics.

Resorting to a non-equilibrium Green function formalism [42, 52, 53, 55, 56] well suited for time-dependent drives, the average power can be written as (see [54], where analogous expressions for the heat currents are also reported)

kernel

$$\tilde{k}_0(\omega) = -i\omega \tilde{\gamma}_2(\omega) + \sum_{n=\pm 2} \tilde{k}_n(\omega); \quad \tilde{k}_{\pm 2}(\omega) = -\frac{i}{4} \omega_\pm \tilde{\gamma}_1(\omega_\pm),$$

with $\tilde{\gamma}_\nu(\omega)$ the Fourier transform of $\gamma_\nu(t)$ in Eq. (3), and $\omega_\pm = \omega \pm \Omega$. The Floquet coefficients possess only even μ components and have the following symmetry properties: $\tilde{G}_\mu^*(\omega) = \tilde{G}_{-\mu}(-\omega)$ and $\tilde{G}_\mu(\omega - \frac{\mu}{2}\Omega) = \tilde{G}_{-\mu}(\omega + \frac{\mu}{2}\Omega)$ [54].

Dynamical heat engine at weak coupling.— As a starting point, we consider the case in which the system/bath

coupling strength of the modulated in time reservoir ($\nu = 1$) is very weak. In terms of spectral functions, this is equivalent to assume $|\mathcal{J}_1(\omega)| \ll |\mathcal{J}_2(\omega)|$. In this regime, it is possible to find closed expressions for the average heat power, from which one can inspect general and necessary conditions to reach a heat engine regime, independently of the precise shape of $\mathcal{J}_1(\omega)$. Up to linear order in $\mathcal{J}_1(\omega)$ the average heat power can be written as [54]:

$$P = -\Omega \int_0^{+\infty} \frac{d\omega}{4\pi m} \text{Im} \chi_0(\omega) f(\omega, \Omega), \quad (8)$$

with $\chi_0(\omega) = -[\omega^2 - \omega_0^2 + i\omega\tilde{\gamma}_2(\omega)]^{-1}$ the bare susceptibility and

$$f(\omega, \Omega) = \mathcal{J}_1(\omega_+) n_B\left(\frac{\omega_+}{T_1}\right) - \mathcal{J}_1(\omega_-) n_B\left(\frac{\omega_-}{T_1}\right) + [\mathcal{J}_1(\omega_-) - \mathcal{J}_1(\omega_+)] n_B\left(\frac{\omega}{T_2}\right), \quad (9)$$

with $n_B(x) = (e^x - 1)^{-1}$ the Bose distribution function. Note that $\mathcal{J}_2(\omega)$ only enters into the expression of $\chi_0(\omega)$ through $\tilde{\gamma}_2(\omega)$ [57]. From Eq. (8), it is possible to find operating conditions for a heat engine, which in our convention corresponds to $P < 0$. First of all, recalling that $\mathcal{J}_2(\omega) = m\omega \text{Re}[\tilde{\gamma}_2(\omega)]$, one can realize that $\text{Im}[\chi_0(\omega)]$ is positive for $\omega > 0$. Therefore, the regions where

$$f(\omega, \Omega) > 0, \quad (10)$$

actually govern the possibility to obtain a heat engine.

We now specialize to a wide class of spectral functions, i.e. monotonically increasing $\mathcal{J}_1(\omega)$. In this case, the last sum that appears in square brackets on the second line of Eq. (9) is always negative, then the most favourable requirement for a working heat engine is in the $T_2 \rightarrow 0$ limit, where the second line vanishes (hence $T_1 > T_2$). Taking advantage of the relation $\tilde{\mathcal{L}}_1(-\omega) = 2\mathcal{J}_1(\omega)n_B(\omega/T_1)$, with $\tilde{\mathcal{L}}_1(\omega)$ Fourier transform of the fluctuating force correlator $\mathcal{L}_1(t)$, we can then recast the condition (10) as

$$\tilde{\mathcal{L}}_1(-\omega - \Omega) > \tilde{\mathcal{L}}_1(-\omega + \Omega). \quad (11)$$

It is now easy to conclude that it is never possible to get a heat engine in the case of Markovian dynamics of the environment connected to the system via a modulated coupling. Indeed, a memoryless bath is described by a fluctuating force correlator $\mathcal{L}_1(t) \propto \delta(t)$, that corresponds to a constant $\tilde{\mathcal{L}}_1(\omega)$, hence inequality (11) is never satisfied, for any value of ω . Therefore, *non-Markovianity is a necessary condition to achieve a working heat engine*. It is worth to underline that, within a microscopic bath description as the one adopted here, the only case with a purely Markovian dynamics is a strictly Ohmic spectral function $\mathcal{J}_1(\omega) = m\gamma_1\omega$ in the classic (high temperature) regime $T_1 \gg \omega_0$, where $\mathcal{L}_1(t) = m\gamma_1 T_1 \delta(t)$ [28].

The above discussion can be generalized to a wider class of spectral densities $\mathcal{J}_1(\omega)$ centered around a characteristic (positive) frequency, say ω_1 , which are relevant in the description of structured non-Markovian environments [58–62]. Here, one always find the possibility for a heat engine. Indeed, under the assumption of a sufficiently sharp peak around ω_1 (of width Δ , with $\Omega > \Delta$) and looking at Eqs. (9)-(10), the dominant contributions are for either $\omega_+ \simeq \omega_1$ or $\omega_- \simeq \omega_1$. In the former case one needs $n_B(\frac{\omega_1}{T_1}) > n_B(\frac{\omega_1 - \Omega}{T_2})$, hence $T_1 > T_2$, while in the latter one has $n_B(\frac{\omega_1 + \Omega}{T_2}) > n_B(\frac{\omega_1}{T_1})$, thus leading to the opposite case $T_1 < T_2$. Therefore, a peaked spectral function provides a wide and flexible parameter window of operation. It is indeed possible to find a working window for the heat engine regime in the two opposite temperature configurations, by properly tuning the external frequency Ω .

To illustrate concretely the above arguments, we consider two paradigmatic examples. For the sake of clarity, we take the simplest case for the $\nu = 2$ bath, i.e. a strictly Ohmic spectral density $\mathcal{J}_2(\omega) = m\gamma_2\omega$ [63], therefore $\chi_0(\omega)$ results peaked around the characteristic frequency ω_0 for sufficiently small $\gamma_2 \ll \omega_0$. Regarding the modulated bath, we first focus on a monotonically increasing spectral density of the form $\mathcal{J}_1(\omega) = m\gamma_1\omega|\frac{\omega}{\omega_0}|^{s-1}$, which describes a large class of spectral function [64]: Ohmic behaviour for $s = 1$, sub-Ohmic for $0 < s < 1$, and super-Ohmic for $s > 1$ [28, 63]. First of all, it is possible to demonstrate [54] that in the case $0 < s \leq 1$ no heat engine can be achieved. Since both the Ohmic case in the quantum regime and the sub-Ohmic case are non-Markovian, we can conclude that *non-Markovianity is a necessary but not sufficient condition to obtain a heat engine*.

On the contrary, the inequality in Eq. (10) can be satisfied in the super-Ohmic case with $s > 1$, hence there a quantum heat engine can always exist. Two representative examples of super-Ohmic spectral functions (with $s = 1.5$ and $s = 3$) are presented in Fig. 2, where as figures of merit we inspect the average power $-P$ and associated efficiency $\eta = -P/J_1$. Firstly, we have checked (not shown) that the optimal performance (in terms of magnitude) are reached in the quantum regime $T_2 \ll \omega_0$ [65]. Increasing T_1 , the average power magnitude increases, with a corresponding widening of the frequency range Ω . Concerning the efficiency, η is an increasing function of T_1 , always limited by $\eta < \eta_C = 1 - T_2/T_1$. A careful analysis [54] allows to conclude that for $1 < s \leq 2$ the maximum efficiency is $\eta = \eta_C/2$ (reached at $\Omega = \omega_0$) for any temperature T_1 . On the other hand, when $s > 2$, the efficiency can exceed $\eta_C/2$ for large enough temperatures T_1 .

We now consider a prototypical example of a non-Markovian structured environment described by a Lorentzian spectral function [58–62] $\mathcal{J}_1(\omega) =$

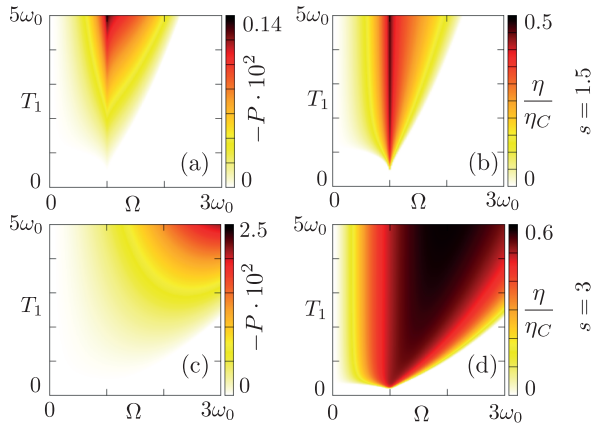


FIG. 2. Density plot of the power $-P$ (in unit of γ_2^2) and efficiency η normalized to the Carnot limit $\eta_C \approx 1$ (see parameters) for a super-Ohmic engine with $s = 1.5$ and $s = 3$, as a function of the driving frequency Ω and of the temperature T_1 (in units of ω_0). Panels (a,b) show the case $s = 1.5$, panels (c,d) the case $s = 3$. In all panels, we set $\gamma_2 = 10^{-2}\omega_0$, $\gamma_1 = 10^{-2}\gamma_2$, $\bar{\omega} = \omega_0$ and $T_2 = 5 \cdot 10^{-3}\omega_0$.

$d_1 m \gamma_1 \omega / [(\omega^2 - \omega_1^2)^2 + \gamma_1^2 \omega^2]$. Such environment can be physically realized for instance with cavity-qed architectures [66–68] (see the sketch in Fig. 3(a)), where the coupling strength d_1 between the QHO and the lossy cavity can be engineered. This spectral function has a peak centered at ω_1 with a width determined by γ_1 (parameter linked to the cavity loss). For clarity we introduce the dimensionless parameter $\kappa \equiv d_1 / (\omega_0^2 \omega_1^2)$, whose value can interpolate between a weak coupling regime ($\kappa \ll 1$), analyzed here, and a strong coupling one ($\kappa \gg 1$) discussed below.

Figures 3(b–e) show the corresponding power and the efficiency for two different temperature arrangements: $T_1 > T_2$ and $T_1 < T_2$. The behaviors of the average power well agree with the necessary conditions discussed above, with the resonance condition $\omega_1 \simeq \omega_0 \pm \Omega$ (see the dashed line in the plots). Indeed, with the chosen parameters in the two cases one expects $\Omega \lesssim 10\omega_0$ and $\Omega \lesssim \omega_0$, respectively [69]. Note that in both cases the maximum power occurs for $\omega_1 = \omega_0 - \Omega \text{sgn}(T_2 - T_1)$. Also in this case, we found that the best condition to increase the power yield of the heat engine is to increase the temperature gradient among the contacts, leading to one of them being in the quantum ($T \ll \omega_0$) and the other in the classic ($T > \omega_0$) regime. With regard to engine efficiency, it is possible to show [54] its maximum can be expressed as $\eta = 1 - \text{Min}[\omega_0, \omega_1] / \text{Max}[\omega_0, \omega_1] < \eta_C$, so that *the Carnot limit can be approached* in a realistic parameter window. Note, however, that maximum power and maximum efficiency are reached at different values of ω_1 . In particular, the latter is achieved for $\omega_1 = \frac{T_1}{T_2}\omega_0$, where the power vanishes.

Heat engine beyond weak coupling.— The results dis-

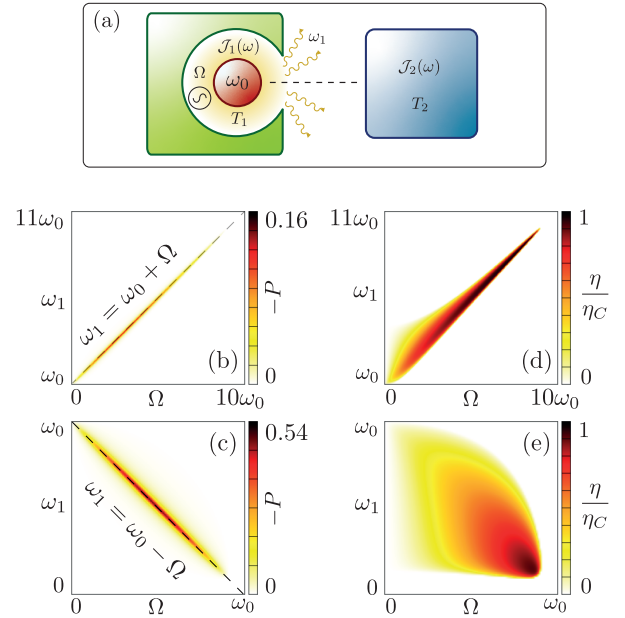


FIG. 3. Heat engine with a structured environment as pictorially depicted in panel(a). Panels (b,c) show the engine average power (in unit of γ_2^2) and panels (d,e) show the engine efficiency normalized to the Carnot limit η/η_C as a function of the driving frequency Ω and the frequency of the peak ω_1 (in units of ω_0). In panels (b,d) we have set $T_1 = 2\omega_0$, $T_2 = 0.2\omega_0$ while in panels (c,e) we have set the opposite configuration with $T_1 = 0.2\omega_0$, $T_2 = 2\omega_0$. Other parameters are $\gamma_1 = 10^{-2}\gamma_2$, $\gamma_2 = 0.01\omega_0$, and $\kappa = 0.001$.

cussed so far have been obtained assuming weak coupling strength for the driven system/bath contact, demonstrating that a dynamical heat engine can be established only in a non-Markovian setting. It is fair to wonder how robust are these results at stronger couplings. To this end, we now consider a strictly Markovian dynamics, demonstrating that it is never possible to obtain a working heat engine in such a case, regardless of the strength of the system/bath coupling. Therefore, we choose an Ohmic spectral function $\mathcal{J}_1(\omega) = m\gamma_1\omega$. In this case, the first line and the first term in the second line of Eq. (6) are always positive [54]. Then, in the search for a heat engine, $P < 0$, we should look for a negative contribution of the remaining term

$$-\frac{\gamma_1 \Omega}{4\pi} \int_{-\infty}^{+\infty} d\omega \coth\left(\frac{\omega}{2T_1}\right) \omega \text{Im}[\tilde{G}_0(\omega - \Omega)].$$

Considering now the Markovian regime where $\coth\left(\frac{\omega}{2T_1}\right) \rightarrow \frac{2T_1}{\omega}$, and using the symmetry properties of $\tilde{G}_0(\omega - \Omega)$ one can recognize that the above integral is strictly zero. This demonstrates, to all orders in the coupling strength, that non-Markovianity is a necessary condition to achieve a working heat engine.

To investigate the heat engine performance beyond weak coupling, we have performed a detailed numerical

study, for the case of a structured Lorentzian spectral density, computing power and efficiency without resorting to any approximation. We have seen (see [54]) that, while the maximum efficiency is achieved at weak coupling $\kappa \ll 1$, the power is a non-monotonous function of κ , with the maximum in the non-perturbative regime. Therefore, the parameter κ can be used to tune the trade-off between power and efficiency of the heat engine.

Conclusions and outlook.— We have shown that non-Markovian dynamics is a useful resource for quantum thermodynamics, in that it allows for efficient dynamical heat engines, even approaching Carnot efficiency, by appropriately modulating the system-bath coupling. Our results open up new possibilities for the exploitation of non-Markovianity. For instance, one could consider the combined effect of modulating couplings and driving the system, looking for a cooperative effect to enhance the performance of thermal machines. In such a quest, machine learning tools [70–74] could prove to be very useful. Regarding possible experimental implementations, our results on structured environment could be tested in the field of cavity optomechanics, which are emerging as an interesting platform for new quantum technologies [68, 75–78]. An interesting follow-up would be to investigate the role of non-Markovian contributions with different working medium, for instance one or more qubits, that can be integrated in cavity-qed architectures [66, 67, 79–81].

Acknowledgements.— F.C. and M.S. acknowledge support by the “Dipartimento di Eccellenza MIUR 2018-2022”. G.B. acknowledges financial support by the the Julian Schwinger Foundation (Grant JSF-21-04-0001) and by INFN through the project “QUANTUM”.

* fabio.cavaliere@fisica.unige.it

- [1] J. P. Pekola, *Nature Phys.* **11**, 118 (2015).
- [2] S. Vinjanampathy and J. Anders, *Contemporary Physics* **57**, 1 (2016).
- [3] G. Benenti, G. Casati, K. Saito, and R. S. Whitney, *Phys. Rep.* **694**, 1 (2017).
- [4] F. Curzon and B. Alhborn, *Am. J. Phys.* **43**, 22 (1975).
- [5] F. Campaioli, F. A. Pollock, and S. Vinjanampathy, *Thermodynamics in the Quantum Regime*, edited by F. Binder, L. A. Correa, C. Gogolin, J. Anders, and G. Adesso, (Springer, Berlin, 2018).
- [6] N. Killoran, S. F. Huelga, and M. Plenio, *J. Chem. Phys.* **143**, 155102 (2015).
- [7] S. Ciliberto, *Phys. Rev. X* **7**, 021051 (2017).
- [8] Q. Bouton, J. Nettersheim, S. Burgard, D. Adam, E. Lutz, and A. Widerra, *Nat. Commun.* **12**, 2063 (2021).
- [9] H. Thierschmann, R. Sanchez, B. Sothmann, F. Arnold, C. Heyn, W. Hansen, H. Buhmann, and L. W. Molenkamp, *Nature Nanotech.* **10**, 854 (2015).
- [10] I. A. Martinez, E. Roldan, L. Dinis, D. Petrov, J. M. R. Parrondo, and R. A. Ríca, *Nat. Phys.* **12**, 67 (2016).
- [11] G. Blasi, F. Taddei, M. Carrega, L. Arrachea, and A. Braggio, *Phys. Rev. B* **103**, 235434 (2021).
- [12] M. Xu, J. T. Stockburger, G. Kurizki, and J. A. Ankerhold, *New J. Phys.* **24**, 035003 (2022).
- [13] M. Esposito, U. Harbola, and S. Mukamel, *Rev. Mod. Phys.* **81**, 1665 (2009).
- [14] M. Campisi, P. Hänggi, and P. Talkner, *Rev. Mod. Phys.* **83**, 771 (2011).
- [15] R. Kosloff, *Entropy* **15**, 2100 (2013).
- [16] D. Gelbwaser-Klimovsky, W. Niedenzu, and G. Kurizki, *Adv. At. Mol. Opt. Phys.* **64**, 329 (2015).
- [17] J. Goold, M. Huber, A. Riera, L. del Rio, and P. Skrzypczyk, *J. Phys. A Math. Theor.* **49**, 1430001 (2016).
- [18] M. Carrega, M. Sassetti, and U. Weiss, *Phys. Rev. A* **99**, 062111 (2019).
- [19] H. J. D. Miller, M. Scandi, J. Anders, and M. Perarnau-Llobet, *Phys. Rev. Lett.* **123**, 230603 (2019).
- [20] S. Khandelwal, N. Palazzo, N. Brunner, and G. Haack, *New J. Phys.* **22**, 073039 (2020).
- [21] F. Vischi, M. Carrega, E. Strambini, P. Virtanen, A. Braggio, and F. Giazotto, *Sci. Rep.* **9**, 3238 (2019).
- [22] B. Bhandari, P. A. Erdman, R. Fazio, E. Paladino, and F. Taddei, *Phys. Rev. B* **103**, 155434 (2021).
- [23] N. Pancotti, M. Scandi, M. T. Mitchison, and M. Perarnau-Llobet, *Phys. Rev. X* **10**, 031015 (2020).
- [24] M. Wiedmann, J. T. Stockburger, and J. Ankerhold, *New J. Phys.* **22**, 033007 (2020).
- [25] J. Liu, K. A. Jung, and D. Segal, *Phys. Rev. Lett.* **127**, 200602 (2022).
- [26] J. Son, P. Talkner, and J. Thingna, *Phys. Rev. X Quantum* **2**, 040328 (2021).
- [27] H.-P. Breuer and F. Petruccione, *The theory of open quantum systems* (Oxford University Press, 2002).
- [28] U. Weiss, *Quantum Dissipative Systems - 5th Edition* (World Scientific, Singapore, 2021).
- [29] E. Aurell, *Phys. Rev. E* **97**, 062117 (2018).
- [30] G. Benenti, G. Casati, D. Rossini, and G. Strini, *Principles of quantum computation and information* (A comprehensive textbook) (World Scientific, Singapore, 2019).
- [31] W. Wang, J. Han, B. Yadin, Y. Ma, J. Ma, W. Cai, Y. Xu, L. Hu, H. Wang, Y. P. Song, M. Gu, and L. Sun, *Phys. Rev. Lett.* **123**, 220501 (2019).
- [32] C. Elouard, G. Thomas, O. Maillet, J. P. Pekola, and A. N. Jordan, *Phys. Rev. E* **102**, 030102 (2020).
- [33] D. Rossini, G. M. Andolina, D. Rosa, M. Carrega, and M. Polini, *Phys. Rev. Lett.* **125**, 236402 (2020).
- [34] J.-E. Gyhm, D. Safranek, and D. Rosa, *Phys. Rev. Lett.* **128**, 140501 (2022).
- [35] G. Watanabe, B. Prasanna Venkatesh, P. Talkner, and A. Del Campo, *Phys. Rev. Lett.* **118**, 050601 (2017).
- [36] G. Watanabe, B. Prasanna Venkatesh, P. Talkner, M.-J. Wang, and A. Del Campo, *Phys. Rev. Lett.* **124**, 210603 (2020).
- [37] K. Hammam, H. Leitch, Y. Assouni, and G. De Chiara, *ArXiv:2202.07515* (2022).
- [38] P. Talkner and P. Hänggi, *Rev. Mod. Phys.* **92**, 41002 (2020).
- [39] I. de Vega and D. Alonso, *Rev. Mod. Phys.* **89**, 015001 (2017).
- [40] G. T. Landi, M. Paternostro, and A. Belenchia, *PRX Quantum* **3**, 010303 (2022).
- [41] A. Hewgill, G. De Chiara, and A. Imparato, *Phys. Rev. Research* **3**, 013165 (2021).
- [42] M. Carrega, L. M. Cangemi, G. De Filippis, V. Cataudella, G. Benenti, and M. Sassetti, *PRX quantum*

- 3**, 010323 (2022).
- [43] F. Ivander, N. Anto-Sztrikacs, and D. Segal, ArXiv:2111.05302 (2021).
- [44] Y. Shirai, K. Ashimoto, R. Tezuka, K. Uchiyama, and N. Atano, Phys. Rev. Research **3**, 023078 (2021).
- [45] S. M. Loos and S. H. L. Klapp, New J. Phys. **22**, 123051 (2020).
- [46] K. Ptaszynski, ArXiv:2203.14671 (2022).
- [47] H. Leitch, N. Piccione, B. Bellomo, and G. De Chiara, AVS Quantum Sci. **4**, 012001 (2022).
- [48] P. P. Hofer, M. Perarnau-Llobet, L. D. M. Miranda, G. Haack, R. Silva, J. Bohr Brask, and N. Brunner, New J. Phys. **19**, 123037 (2017).
- [49] A. O. Caldeira and A. J. Leggett, Ann. Phys. **149**, 374 (1983).
- [50] L. M. Cangemi, M. Carrega, A. De Candia, V. Cataudella, G. De Filippis, M. Sassetti, and G. Benenti, Phys. Rev. Research **3**, 013237 (2021).
- [51] P. Portugal, C. Flindt, and N. Lo Gullo, Phys. Rev. B **104**, 205420 (2021).
- [52] N. Freitas and J. P. Paz, Phys. Rev. E **95**, 012146 (2017).
- [53] N. Freitas and J. P. Paz, Phys. Rev. A **97**, 032104 (2018).
- [54] See supplemental material.
- [55] L. Arrachea, E. Mucciolo, C. Chamon, and R. Capaz, Phys. Rev. B **86**, 125424 (2012).
- [56] M. Grifoni, M. Sassetti, P. Hanggi, and U. Weiss, Phys. Rev. E **52**, 3596 (1995).
- [57] Due to the perturbative expansion, $\tilde{\gamma}_2(\omega)$ is the only contribution from $\tilde{k}_0(\omega)$ that enters Eq. (8), $\tilde{\gamma}_1(\omega)$ having been discarded.
- [58] M. Thorwart, E. Paladino, and M. Grifoni, Chem. Phys. **296**, 333 (2004).
- [59] E. Paladino, A. G. Mauger, M. Sassetti, G. Falci, and U. Weiss, Physica E **40**, 198 (2007).
- [60] M. C. Goorden, M. Thorwart, and M. Grifoni, Eur. Phys. J. B **45**, 405 (2005).
- [61] L. Magazzu, P. Forn-Diaz, R. Belyansky, J.-L. Orgiazzi, M. A. Yurtalan, M. R. Otto, A. Lupascu, C. M. Wilson, and M. Grifoni, Nat. Commun. **9**, 1403 (2018).
- [62] J. Iles-Smith, N. Lambert, and A. Nazir Phys. Rev. A **90**, 032114 (2014).
- [63] Note that we have assumed the usual cut-off ω_c as the largest energy scale, i.e. $\omega_c \gg \omega_0, \Omega$.
- [64] A generalization to the case of finite and small cut-off $\omega_c \lesssim 2\omega_0$ can be found in [54]. There, it is possible to obtain a working heat engine also in the case of $s \leq 1$.
- [65] We underline that a working heat engine exists also for $\omega_0 < T_2 < T_1$, with both temperature in the classic regime.
- [66] A. Cottet, M. C. Dartiaill, M. M. Desjardins, T. Cubaynes, L. C. Contamin, M. Delbec, J. J. Viennot, L. E. Bruhat, B. Doucot, and T. Kontos, J. Phys.: Condens. Matter **29**, 433002 (2017).
- [67] M. Scigliuzzo, A. Bengtsson, J.-C. Besse, A. Wallraff, P. Delsing, and S. Gasparinetti, Phys. Rev. X **10**, 041054 (2020).
- [68] S. Barzanjeh, A. Xuereb, S. Gröblacher, M. Paternostro, C. A. Regal, and E. Weig, Nat. Phys. **18**, 15 (2022).
- [69] A small broadening of the resonances is due to the damping factors γ_1, γ_2 .
- [70] M. M. Müller, R. S. Said, F. Jelezko, T. Calarco, and S. Montangero, arXiv:2104.07687 (2021).
- [71] V. Cavina, A. Mari, A. Carlini, and V. Giovannetti, Phys. Rev. A **98**, 052125 (2018).
- [72] G. Manzano, F. Plastina, and R. Zambrini, Phys. Rev. Lett. **121**, 120602 (2018).
- [73] P. A. Erdman and F. Noe, NPJ Quantum Inf. **8**, 1 (2022).
- [74] I. Khait, J. Carrasquilla, and D. Segal, Phys. Rev. Research **4**, L012029 (2022).
- [75] S. Barzanjeh, M. Aquilina, and A. Xuereb, Phys. Rev. Lett. **120**, 060601 (2018).
- [76] B. Nair, A. Xuereb, and A. Dantan, Phys. Rev. A **94**, 053812 (2016).
- [77] A. Pontin, H. Fu, J. Iacoponi, P. F. Barker, and T. S. Monteiro, ArXiv:2204.09625 (2022).
- [78] B. Maas, D. Hartley, K. Busch, and D. Rázal, ArXiv:2111.10163 (2021).
- [79] J. J. Viennot, M. C. Dartiaill, A. Cottet, and T. Kontos, Science **349**, 408 (2015).
- [80] Y. Lu, A. Bengtsson, J. J. Burnet, E. Wiegand, B. Suri, P. Krantz, A. Fadavi Roudsari, A. F. Kockum, S. Gasparinetti, G. Johansson, P. Delsing, NPJ Quantum Information **7**, 35 (2021).
- [81] Y. Lu, N. Lambert, A. F. Kockum, K. Funo, A. Bengtsson, S. Gasparinetti, F. Nori, and P. Delsing, PRX Quantum **3**, 020305 (2022).
- [82] In general, this shift will bring the set $\mathcal{P}(\bar{\mu}, n)$ but this does not constitute a problem since the mathematical expressions associated to the sum over all paths are still valid.
- [83] Of course this does not imply that the maximum power and maximum efficiency conditions for a super-Ohmic engine are given for the same set of parameters s, Ω, T_1 .
- [84] Note that for $0 < \Omega < \omega_c - \omega_0$ and $\Omega > \omega_c + \omega_0$ one has $\theta(\omega_c - |\omega_0 + p\Omega|) \neq 0$ for both $p = \pm 1$: this case behaves as the $s = 1$ case discussed previously and gives $P > 0$.
- [85] All results have been obtained adopting standard linear algebra and series acceleration packages in a in-house developed highly parallel code.

General framework

Here we remind the general setting and some useful definitions. The working medium is connected to two reservoirs, in equilibrium at temperature T_1 and T_2 , respectively. We remind that the total Hamiltonian is

$$H^{(t)} = H_{\text{QHO}} + \sum_{\nu=1}^2 \left[H_{\nu} + H_{\text{int},\nu}^{(t)} \right], \quad (1)$$

with the quantum harmonic oscillator (QHO) and the bath oscillators given respectively by

$$H_{\text{QHO}} = \frac{p^2}{2m} + \frac{1}{2}m\omega_0^2 x^2, \quad H_{\nu} = \sum_{k=1}^{\infty} \left[\frac{P_{k,\nu}^2}{2m_{k,\nu}} + \frac{m_{k,\nu}\omega_{k,\nu}^2 X_{k,\nu}^2}{2} \right]. \quad (2)$$

We consider a general framework where the system/bath couplings are modulated in time with periodic functions $g_{\nu}(t) = g_{\nu}(t + \mathcal{T})$ with series decomposition

$$g_{\nu}(t) = \sum_{n=-\infty}^{+\infty} g_{n,\nu} e^{-in\Omega t}, \quad \Omega = \frac{2\pi}{\mathcal{T}}. \quad (3)$$

The total system/bath interaction is given by

$$H_{\text{int}}^{(t)} = \sum_{\nu=1}^2 H_{\text{int},\nu}^{(t)} = \sum_{\nu=1}^2 \sum_{k=1}^{\infty} \left\{ -x g_{\nu}(t) c_{k,\nu} X_{k,\nu} + x^2 g_{\nu}^2(t) \frac{c_{k,\nu}^2}{2m_{k,\nu}\omega_{k,\nu}^2} \right\}, \quad (4)$$

where the subscript t indicates the parametric time dependence in the couplings $g_{\nu}(t)$. Using the total Hamiltonian, the equations of motion (EOM) for the QHO operators ($x(t), p(t)$) and for the baths oscillator operators ($X_{k,\nu}(t), P_{k,\nu}(t)$) are

$$\dot{x}(t) = \frac{p(t)}{m}, \quad \dot{p}(t) = -m\omega_0^2 x(t) + \sum_{\nu=1}^2 \sum_{k=1}^{\infty} g_{\nu}(t) c_{k,\nu} \left[X_{k,\nu}(t) - \frac{g_{\nu}(t) c_{k,\nu}}{m_{k,\nu}\omega_{k,\nu}^2} x(t) \right], \quad (5)$$

and

$$\dot{X}_{k,\nu}(t) = \frac{P_{k,\nu}(t)}{m_{k,\nu}}, \quad \dot{P}_{k,\nu}(t) = -m_{k,\nu}\omega_{k,\nu}^2 X_{k,\nu}(t) + g_{\nu}(t) c_{k,\nu} x(t). \quad (6)$$

The bath dynamics can be solved in terms of the position of the QHO, which will fulfill the generalized quantum Langevin equation [42] quoted in Eq.(3) of the main part. The solution of the Langevin equation is obtained with the knowledge of the retarded Green function $G(t, t')$ which obeys:

$$\ddot{G}(t, t') + \omega_0^2 G(t, t') + \int_{t_0}^{+\infty} ds \sum_{\nu=1}^2 g_{\nu}(t) \gamma_{\nu}(t-s) [\dot{g}_{\nu}(s) G(s, t') + g_{\nu}(s) \dot{G}(s, t')] = \delta(t - t'), \quad (7)$$

where the dot denotes the derivative with respect to the first argument and $G(t, t') = 0$ for $t \leq t'$. Here, $t_0 \rightarrow -\infty$ is the initial time and the memory damping is

$$\gamma_{\nu}(t) = \frac{\theta(t)}{m} \sum_{k=1}^{\infty} \frac{c_{k,\nu}^2}{m_{k,\nu}\omega_{k,\nu}^2} \cos(\omega_{k,\nu} t), \quad (8)$$

which is linked to the spectral density $\mathcal{J}_{\nu}(\omega) = \frac{\pi}{2} \sum_{k=1}^{\infty} \frac{c_{k,\nu}^2}{m_{k,\nu}\omega_{k,\nu}} \delta(\omega - \omega_{k,\nu})$ via [28]

$$\gamma_{\nu}(t) = \frac{2}{\pi m} \theta(t) \int_0^{\infty} d\omega \frac{\mathcal{J}_{\nu}(\omega)}{\omega} \cos(\omega t). \quad (9)$$

At long times, when the memory of the initial state for the QHO is lost, the time evolution of the position operator $x(t)$ is directly expressed as a time integral of the retarded Green function as:

$$x(t) = \frac{1}{m} \lim_{t_0 \rightarrow -\infty} \int_{t_0}^{+\infty} dt' G(t, t') \sum_{\nu=1}^2 g_{\nu}(t') \xi_{\nu}(t'), \quad (10)$$

where

$$\xi_\nu(t) = \sum_{k=1}^{\infty} c_{k,\nu} [X_{k,\nu}(t_0) \cos \omega_{k,\nu}(t - t_0) + \frac{P_{k,\nu}(t_0)}{m_{k,\nu} \omega_{k,\nu}} \sin \omega_{k,\nu}(t - t_0)] \quad (11)$$

is the fluctuating force of the bath ν , and it depends explicitly on the initial values of the bath position/momentum operators $X_{k,\nu}(t_0)$ and $P_{k,\nu}(t_0)$. It has zero quantum average, $\text{Tr}[\xi_\nu(t)\rho(t_0)] = 0$, and correlator

$$\text{Tr}[\xi_\nu(t)\xi_{\nu'}(t')\rho(t_0)] \equiv \langle \xi_\nu(t)\xi_{\nu'}(t') \rangle = \delta_{\nu,\nu'} \mathcal{L}_\nu(t - t') = \delta_{\nu,\nu'} \int_0^\infty \frac{d\omega}{\pi} \mathcal{J}_\nu(\omega) \left[\coth\left(\frac{\omega}{2T_\nu}\right) \cos(\omega t) - i \sin(\omega t) \right]. \quad (12)$$

As we will see shortly, the key relation (10) will allow us to evaluate all quantum correlation averages, associated to thermodynamical observables. Notice that at long times $G(t, t')$ acquires the following peculiar form:

$$G(t, t') = \sum_{\mu=-\infty}^{+\infty} \int_{-\infty}^{+\infty} \frac{d\omega}{2\pi} e^{-i\omega(t-t')} \tilde{G}_\mu(\omega) e^{-i\mu\Omega t}, \quad (13)$$

where $\tilde{G}_\mu(\omega)$ are the so-called Floquet coefficients obeying to the following algebraic set of equations [42]:

$$\tilde{G}_\mu(\omega) = \chi(\omega) \delta_{\mu,0} - \chi(\omega + \mu\Omega) \sum_{n \neq 0} \tilde{k}_n(\omega + (\mu - n)\Omega) \tilde{G}_{\mu-n}(\omega). \quad (14)$$

Here,

$$\chi(\omega) = -\frac{1}{\omega^2 - \omega_0^2 - \tilde{k}_0(\omega)} \quad \text{and} \quad \tilde{k}_n(\omega) = -i \sum_{\nu=1}^2 \sum_{\mu=-\infty}^{+\infty} g_{\mu,\nu} g_{n-\mu,\nu}(\omega + \mu\Omega) \tilde{\gamma}_\nu(\omega + \mu\Omega). \quad (15)$$

Average thermodynamic quantities

We now focus on the evaluation of the long time behaviour of thermodynamic quantities. We start considering the Heisenberg time evolution $O^{(t)}(t) = \mathcal{U}^\dagger(t, t_0) O^{(t)} \mathcal{U}(t, t_0)$ of a given operator $O^{(t)}$, with $\mathcal{U}(t, t_0)$ the time evolution operator of the total Hamiltonian $H^{(t)}$. The corresponding quantum average is

$$\langle O^{(t)}(t) \rangle \equiv \text{Tr}[O^{(t)}(t)\rho(t_0)] = \text{Tr}[O^{(t)}\rho(t)], \quad (16)$$

where we recall that the apex $O^{(t)}$ indicates the possible explicit time dependence of the operator O (in our case due to the time dependent system/bath couplings). Notice that the trace is done over the initial density matrix $\rho(t_0 \rightarrow -\infty)$ which is assumed to consist of uncoupled system and baths. Due to the cyclic property of the trace, one can shift the time dependence into the total density matrix $\rho(t) = \mathcal{U}(t, t_0)\rho(t_0)\mathcal{U}^\dagger(t, t_0)$ (last equality in Eq. (16)).

In presence of periodic drivings, the thermodynamic quantities are defined with the additional average over the period \mathcal{T} of the cycle. The final mean value of the operator $O^{(t)}(t)$ thus reads

$$O = \frac{1}{\mathcal{T}} \int_t^{t+\mathcal{T}} dt' \langle O^{(t')}(t') \rangle. \quad (17)$$

In the following we will demonstrate that at long times t the above cycling average will be independent of t itself. We start by considering the operatorial time evolution of the total Hamiltonian (1). We have

$$\frac{d}{dt} H^{(t)}(t) = \frac{\partial}{\partial t} H^{(t)}(t) = \sum_{\nu=1}^2 \frac{\partial}{\partial t} H_{\text{int},\nu}^{(t)}(t) = \sum_{\nu=1}^2 P_\nu(t) = P(t), \quad (18)$$

where we denoted with $P_\nu(t)$ the power operator associated to the temporal variation of the system/bath coupling $g_\nu(t)$ and with $P(t)$ the total power contribution. The corresponding time-dependent heat current, associated to the ν -th bath, is given by the change in time of the reservoir energy:

$$J_\nu(t) = -\frac{d}{dt} H_\nu(t), \quad (19)$$

where the minus sign implies a positive $J_\nu(t)$ when the energy flows from the reservoir into the quantum system. Considering the explicit form (1) of the total Hamiltonian and the relation (18) we arrive to the energy balance relation (still written at an operatorial level):

$$P(t) = - \sum_{\nu=1}^2 J_\nu(t) + \frac{d}{dt} [H_{\text{QHO}}(t) + H_{\text{int}}^{(t)}(t)]. \quad (20)$$

The corresponding quantum ensemble and cycling averages give the following result:

$$P + \sum_{\nu=1}^2 J_\nu(t) = \mathcal{A}, \quad (21)$$

where

$$P = \frac{1}{\mathcal{T}} \int_t^{t+\mathcal{T}} dt' \sum_{\nu=1}^2 \text{Tr} \left[\frac{\partial H_{\text{int},\nu}^{(t')}(t')}{\partial t'} \rho(t_0) \right] = \frac{1}{\mathcal{T}} \int_t^{t+\mathcal{T}} dt' \sum_{\nu=1}^2 \text{Tr} \left[\frac{\partial H_{\text{int},\nu}^{(t')}(t')}{\partial t'} \rho(t') \right], \quad (22)$$

$$J_\nu = - \frac{1}{\mathcal{T}} \int_t^{t+\mathcal{T}} dt' \text{Tr} \left[\frac{d}{dt'} H_\nu(t') \rho(t_0) \right] = - \frac{1}{\mathcal{T}} \int_t^{t+\mathcal{T}} dt' \text{Tr} \left[H_\nu \frac{d}{dt'} \rho(t') \right], \quad (23)$$

$$\mathcal{A} = \frac{1}{\mathcal{T}} \int_t^{t+\mathcal{T}} dt' \text{Tr} \left[\frac{d}{dt'} (H_{\text{QHO}}(t') + H_{\text{int}}^{(t')}(t')) \rho(t_0) \right] = \frac{1}{\mathcal{T}} \int_t^{t+\mathcal{T}} dt' \text{Tr} \left[(H_{\text{QHO}} + H_{\text{int}}^{(t')}(t')) \frac{d}{dt'} \rho(t') \right]. \quad (24)$$

It has been argued [25] that, in general, the term \mathcal{A} can be non-zero. Here, however, we will show that in our case indeed $\mathcal{A} = 0$. This important result implies that in the long time limit and after the cycling average the total power injected from the coupling drives is totally balanced by the reservoir heat currents and it fulfills the relation

$$P + \sum_{\nu=1}^2 J_\nu = 0. \quad (25)$$

To this end, it is convenient to rewrite \mathcal{A} as

$$\mathcal{A} = \frac{1}{\mathcal{T}} \left[\langle H_{\text{int}}^{(t+\mathcal{T})}(t+\mathcal{T}) \rangle - \langle H_{\text{int}}^{(t)}(t) \rangle + \langle H_{\text{QHO}}(t+\mathcal{T}) \rangle - \langle H_{\text{QHO}}(t) \rangle \right]. \quad (26)$$

To demonstrate that $\mathcal{A} = 0$ it is then enough to show that $\langle H_{\text{int}}^{(t)}(t) \rangle$ and $\langle H_{\text{QHO}}(t) \rangle$ are periodic function with period \mathcal{T} . This will be done below. The time dependence of the interaction term operator in Eq. (4) is given by

$$H_{\text{int}}^{(t)}(t) = -x(t) \sum_{\nu=1}^2 \sum_{k=1}^{\infty} g_\nu(t) c_{k,\nu} X_{k,\nu}(t) + x^2(t) \sum_{\nu=1}^2 \sum_{k=1}^{\infty} g_\nu^2(t) \frac{c_{k,\nu}^2}{2m_{k,\nu} \omega_{k,\nu}^2}. \quad (27)$$

Using the equations of motion of the QHO operators in Eq. (5) we can rewrite $H_{\text{int}}^{(t)}(t)$ in terms of the system position operators $x(t)$ as

$$H_{\text{int}}^{(t)}(t) = -m x(t) \frac{d^2}{dt^2} x(t) - x^2(t) \left[m \omega_0^2 + \sum_{\nu=1}^2 \sum_{k=1}^{\infty} g_\nu^2(t) \frac{c_{k,\nu}^2}{2m_{k,\nu} \omega_{k,\nu}^2} \right]. \quad (28)$$

For the QHO term in Eq. (2) we have $H_{\text{QHO}}(t) = \frac{m}{2} \left(\frac{d}{dt} x(t) \right)^2 + \frac{m \omega_0^2}{2} x^2(t)$. The above expressions show that the quantum ensemble average of these terms can be written as correlators of *only* the system position operator. Indeed we have

$$\langle H_{\text{int}}^{(t)}(t) \rangle = -m M_{x\ddot{x}}(t) - \left[m \omega_0^2 + \sum_{\nu=1}^2 \sum_{k=1}^{\infty} g_\nu^2(t) \frac{c_{k,\nu}^2}{2m_{k,\nu} \omega_{k,\nu}^2} \right] M_{xx}(t), \quad \langle H_{\text{QHO}}(t) \rangle = \frac{m}{2} M_{\dot{x}\dot{x}}(t) + \frac{m \omega_0^2}{2} M_{xx}(t), \quad (29)$$

written in terms of three different system position correlators:

$$M_{xx}(t) = \text{Tr} \left[x(t) x(t) \rho(t_0) \right], \quad M_{x\ddot{x}}(t) = \text{Tr} \left[x(t) \frac{d^2}{dt^2} x(t) \rho(t_0) \right], \quad M_{\dot{x}\dot{x}}(t) = \text{Tr} \left[\left(\frac{d}{dt} x(t) \right) \left(\frac{d}{dt} x(t) \right) \rho(t_0) \right]. \quad (30)$$

Notice that these correlators can be represented in terms of the function

$$M(t, s) = \text{Tr} \left[x(t)x(s)\rho(t_0) \right] \quad (31)$$

as:

$$M_{xx}(t) = \lim_{s \rightarrow t} M(t, s), \quad M_{x\ddot{x}}(t) = \lim_{s \rightarrow t} \frac{d^2}{ds^2} M(t, s), \quad M_{\ddot{x}x}(t) = \lim_{s \rightarrow t} \frac{d}{dt} \frac{d}{ds} M(t, s). \quad (32)$$

We then focus on the evaluation of the quantum average of $M(t, s)$. Let us start to insert into (31) the time evolution (10) for $x(t)$ and $x(s)$. We have

$$\begin{aligned} M(t, s) &= \frac{1}{m^2} \int_{-\infty}^{+\infty} dt_1 \int_{-\infty}^{+\infty} dt_2 G(t, t_1) G(s, t_2) \sum_{\nu=1}^2 \sum_{\nu'=1}^2 g_\nu(t_1) g_{\nu'}(t_2) \langle \xi_\nu(t_1) \xi_{\nu'}(t_2) \rangle \\ &= \frac{1}{m^2} \int_{-\infty}^{+\infty} dt_1 \int_{-\infty}^{+\infty} dt_2 G(t, t_1) G(s, t_2) \sum_{\nu=1}^2 g_\nu(t_1) g_\nu(t_2) \mathcal{L}_\nu(t_1 - t_2), \end{aligned} \quad (33)$$

where in the second equality we have inserted the bath correlator given in Eq. (12). The time integrals are solved by using the Fourier representations: Eq. (13) for the Green functions $G(t, t_1)$ and $G(s, t_2)$, Eq. (3) for the driving $g_\nu(t_1)$ and $g_\nu(t_2)$, and for the correlator $\mathcal{L}_\nu(t_1 - t_2) = \int_{-\infty}^{+\infty} \frac{d\omega}{2\pi} e^{-i\omega(t_1 - t_2)} \tilde{\mathcal{L}}_\nu(\omega)$. We obtain

$$M(t, s) = \sum_{n_1, n_2, \mu_1, \mu_2 = -\infty}^{+\infty} \sum_{\nu=1}^2 \int_{-\infty}^{+\infty} \frac{d\omega}{2\pi m^2} \tilde{\mathcal{L}}_\nu(\omega) \tilde{G}_{\mu_2}(-\omega + n_2 \Omega) \tilde{G}_{\mu_1}(\omega + n_1 \Omega) e^{-it(\omega + (n_1 + \mu_1)\Omega)} e^{is(\omega - (n_2 + \mu_2)\Omega)}. \quad (34)$$

Notice that the times t and s are now present only in the exponential factors. This means that after performing the appropriated t and s derivatives, given in the definitions (32), the limit $s \rightarrow t$ implies a time dependent part always of the form $e^{-i\Omega t(n_1 + n_2 + \mu_1 + \mu_2)}$. This shows a clear periodicity with respect to the cycle time \mathcal{T} .

This result demonstrates the periodic properties of the correlators in Eq. (32), namely $M_{xx}(t + \mathcal{T}) = M_{xx}(t)$, $M_{x\ddot{x}}(t + \mathcal{T}) = M_{x\ddot{x}}(t)$ and $M_{\ddot{x}x}(t + \mathcal{T}) = M_{\ddot{x}x}(t)$. Since these correlators are the building blocks of $\langle H_{\text{int}}^{(t)} \rangle$ and $\langle H_{\text{QHO}}(t) \rangle$ we arrive to the conclusion that the quantum averages of the interaction term and of the QHO part are *periodic*.

This eventually demonstrates the key result that $\mathcal{A} = 0$ and then that the cycling average of the total power is totally balanced *only* by the reservoir heat currents – see Eq. (25).

We conclude this part by recalling the general expressions of the average power P_ν and heat current J_ν obtained after performing the averages Eq. (22) and Eq. (23) (see Ref. [42] for the full derivation). We have:

$$\begin{aligned} P_\nu &= \Omega \sum_{n_1, n_2 = -\infty}^{+\infty} n_1 g_{n_1, \nu} g_{n_2, \nu} \int_{-\infty}^{+\infty} \frac{d\omega}{2\pi m} \left\{ i \mathcal{J}_\nu(\omega) \coth\left(\frac{\omega}{2T_\nu}\right) \tilde{G}_{-(n_1 + n_2)}(\omega + n_2 \Omega) \right. \\ &+ \left. \sum_{\nu_1=1}^2 \sum_{\mu=-\infty}^{+\infty} \sum_{n_3, n_4 = -\infty}^{+\infty} g_{n_3, \nu_1} g_{n_4, \nu_1} \frac{\mathcal{J}_{\nu_1}(\omega)}{m} \coth\left(\frac{\omega}{2T_{\nu_1}}\right) \mathcal{J}_\nu(\omega - \Omega(n_2 + n_4 + \mu)) \tilde{G}_\mu(-\omega + n_4 \Omega) \tilde{G}_{-(n_{\text{tot}} + \mu)}(\omega + n_3 \Omega) \right\} \end{aligned} \quad (35)$$

and

$$\begin{aligned} J_\nu &= \sum_{n_1, n_2 = -\infty}^{+\infty} g_{n_1, \nu} g_{n_2, \nu} \int_{-\infty}^{+\infty} \frac{d\omega}{2\pi m} \left\{ -i \mathcal{J}_\nu(\omega) \omega \coth\left(\frac{\omega}{2T_\nu}\right) \tilde{G}_{-(n_1 + n_2)}(\omega + n_2 \Omega) - \sum_{\nu_1=1}^2 \sum_{\mu=-\infty}^{+\infty} \sum_{n_3, n_4 = -\infty}^{+\infty} g_{n_3, \nu_1} g_{n_4, \nu_1} \frac{\mathcal{J}_{\nu_1}(\omega)}{m} \right. \\ &\times \left. \coth\left(\frac{\omega}{2T_{\nu_1}}\right) [\omega - \Omega(n_2 + n_4 + \mu)] \mathcal{J}_\nu(\omega - \Omega(n_2 + n_4 + \mu)) \tilde{G}_{m_1}(-\omega + n_4 \Omega) \tilde{G}_{-(n_{\text{tot}} + \mu)}(\omega + n_3 \Omega) \right\}, \end{aligned} \quad (36)$$

with $n_{\text{tot}} = n_1 + n_2 + n_3 + n_4$. We remind that the spectral functions $\mathcal{J}_\nu(\omega)$ are odd.

Average power and heat currents for a monochromatic drive

We derive here a more compact form for the power and heat currents by focusing on the case discussed in the main part, namely the bath $\nu = 2$ kept constant, while $\nu = 1$ modulated in time with a monochromatic drive

$$g_1(t) = \cos(\Omega t), \quad g_2(t) = 1. \quad (37)$$

Using these explicit forms, with Fourier coefficients $g_{n,1} = (\delta_{n,1} + \delta_{n,-1})/2$ and $g_{n,2} = \delta_{n,0}$, Eq. (15) reduces to

$$\tilde{k}_0(\omega) = -i\omega\tilde{\gamma}_2(\omega) + \sum_{n=\pm 2} \tilde{k}_n(\omega); \quad \tilde{k}_{\pm 2}(\omega) = -\frac{i}{4}\omega_{\pm}\tilde{\gamma}_1(\omega_{\pm}) \quad (38)$$

with $\omega_{\pm} = \omega \pm \Omega$, showing that only the kernels $\tilde{k}_{0,\pm 2}(\omega)$ are different from zero. We now plug the expressions of $g_{\nu}(t)$ into Eq. (37) to write down the average power. First of all, we note that only $g_1(t)$ has a time dependence, hence $P \equiv P_{\nu=1}$, which is conveniently decomposed into two contributions $P = P^{(a)} + P^{(b)}$, where

$$P^{(a)} = -\frac{\Omega}{4\pi m} \int_{-\infty}^{+\infty} d\omega \mathcal{J}_1(\omega) \coth\left(\frac{\omega}{2T_1}\right) \text{Im} \left[\tilde{G}_0(\omega - \Omega) - \tilde{G}_2(\omega - \Omega) \right] \quad (39)$$

and

$$P^{(b)} = \Omega \sum_{n_1, n_2 = -\infty}^{\infty} n_1 g_{n_1,1} g_{n_2,1} \sum_{n_3, n_4 = -\infty}^{+\infty} \sum_{\nu_1=1}^2 g_{n_3, \nu_1} g_{n_4, \nu_1} \sum_{\mu = -\infty}^{+\infty} \int_{-\infty}^{+\infty} \frac{d\omega}{2\pi m^2} \mathcal{J}_{\nu_1}(\omega) \coth\left(\frac{\omega}{2T_{\nu_1}}\right) \\ \times \mathcal{J}_1(\omega - \Omega(n_2 + n_4 + \mu)) \tilde{G}_{\mu}(-\omega + n_4\Omega) \tilde{G}_{-(n_{\text{tot}} + \mu)}(\omega + n_3\Omega). \quad (40)$$

In Eq. (39), we have used that $n_1, n_2 = \pm 1$, and the property of the Floquet coefficients

$$\tilde{G}_{\mu}(\omega) = \tilde{G}_{-\mu}^*(-\omega). \quad (41)$$

In addition, due to the symmetry property (see Sec. for details)

$$\tilde{G}_{\mu}\left(\omega - \frac{\mu}{2}\Omega\right) = \tilde{G}_{-\mu}\left(\omega + \frac{\mu}{2}\Omega\right) \quad (42)$$

the last term in the square brackets of Eq. (39), upon integration, has a null contribution and we can thus write

$$P^{(a)} = -\frac{\Omega}{4\pi m} \int_{-\infty}^{+\infty} d\omega \mathcal{J}_1(\omega) \coth\left(\frac{\omega}{2T_1}\right) \text{Im} \left[\tilde{G}_0(\omega - \Omega) \right]. \quad (43)$$

Using Eq. (41) and renaming $\mu + n_2 + n_4 \rightarrow \mu$ we can rewrite Eq. (40) as

$$P^{(b)} = \frac{\Omega}{2\pi m^2} \sum_{n_1, n_2 = -\infty}^{\infty} n_1 g_{n_1,1} g_{n_2,1} \sum_{n_3, n_4 = -\infty}^{+\infty} \sum_{\nu_1=1}^2 g_{n_3, \nu_1} g_{n_4, \nu_1} \sum_{\mu = -\infty}^{+\infty} \int_{-\infty}^{+\infty} d\omega \mathcal{J}_{\nu_1}(\omega) \coth\left(\frac{\omega}{2T_{\nu_1}}\right) \\ \times \mathcal{J}_1(\omega - \mu\Omega) \text{Re} \left[\tilde{G}_{\mu-(n_2+n_4)}(-\omega + n_4\Omega) \tilde{G}_{-(\mu+n_1+n_3)}(\omega + n_3\Omega) \right].$$

We now insert the explicit form of $g_{n,\nu}$, and for notational convenience we separate $P^{(b)}$ into two contributions $P^{(b,1)} + P^{(b,2)}$ corresponding to the $\nu_1 = 1, 2$ terms in the above expression. The former contribution reads

$$P^{(b,1)} = \frac{\Omega}{32\pi m^2} \int_{-\infty}^{+\infty} d\omega \mathcal{J}_1(\omega) \coth\left(\frac{\omega}{2T_1}\right) \sum_{\mu = -\infty}^{+\infty} \mathcal{J}_1(\omega - \mu\Omega) \text{Re} \left[\sum_{n_1, n_3 = \pm 1} n_1 \tilde{G}_{-(\mu+n_1+n_3)}(\omega + n_3\Omega) \right. \\ \left. \times \sum_{n_2, n_4 = \pm 1} \tilde{G}_{\mu-(n_2+n_4)}(-\omega + n_4\Omega) \right]. \quad (44)$$

Performing the real part of the sum in the last square bracket, using again Eq. (41), one has

$$P^{(b,1)} = \frac{\Omega}{16\pi m^2} \int_{-\infty}^{+\infty} d\omega \mathcal{J}_1(\omega) \coth\left(\frac{\omega}{2T_1}\right) \sum_{\mu = -\infty}^{+\infty} \mathcal{J}_1(\omega - \mu\Omega) |\tilde{G}_{\mu}(-\omega + \Omega) + \tilde{G}_{\mu+2}(-\omega - \Omega)|^2. \quad (45)$$

We now consider $P^{(b,2)}$ related to the $\nu_1 = 2$ contribution in Eq. (40), where $n_1, n_2 = \pm 1$ and $n_3 = n_4 = 0$:

$$P^{(b,2)} = \frac{\Omega}{8\pi m^2} \int_{-\infty}^{+\infty} d\omega \mathcal{J}_2(\omega) \coth\left(\frac{\omega}{2T_2}\right) \sum_{\mu = -\infty}^{+\infty} \mathcal{J}_1(\omega - \mu\Omega) \text{Re} \left[\sum_{n_1, n_2 = \pm 1} n_1 \tilde{G}_{\mu-n_2}(-\omega) \tilde{G}_{-(\mu+n_1)}(\omega) \right].$$

Performing the sum over n_1, n_2 , we arrive at

$$P^{(b,2)} = \frac{\Omega}{8\pi m^2} \int_{-\infty}^{+\infty} d\omega \mathcal{J}_2(\omega) \coth\left(\frac{\omega}{2T_2}\right) \sum_{\mu=-\infty}^{+\infty} |\tilde{G}_\mu(\omega)|^2 \left[\mathcal{J}_1(\omega + (\mu + 1)\Omega) - \mathcal{J}_1(\omega + (\mu - 1)\Omega) \right]. \quad (46)$$

Finally, we sum the three contributions in Eqs. (43), (45), (46) to obtain the expression for the average power $P = P^{(a)} + P^{(b,1)} + P^{(b,2)}$ as reported in Eq.(6) of the main text.

We now conclude this part by analyzing the average heat current J_2 in Eq. (36). We recall that the average heat current J_1 , associated to the other reservoir $\nu = 1$, can be obtained from the energy conservation relation $J_1 = -(P + J_2)$. As above, we separate $J_2 = J_2^{(a)} + J_2^{(b)}$ into two contributions, where

$$J_2^{(a)} = \frac{1}{2\pi m} \int_{-\infty}^{+\infty} d\omega \omega \mathcal{J}_2(\omega) \coth\left(\frac{\omega}{2T_2}\right) \text{Im} \left[\tilde{G}_0(\omega) \right] \quad (47)$$

and

$$J_2^{(b)} = - \sum_{n_1, n_2=-\infty}^{\infty} g_{n_1,2} g_{n_2,2} \sum_{n_3, n_4=-\infty}^{+\infty} \sum_{\nu_1=1}^2 g_{n_3, \nu_1} g_{n_4, \nu_1} \sum_{\mu=-\infty}^{+\infty} \int_{-\infty}^{+\infty} \frac{d\omega}{2\pi m^2} \mathcal{J}_{\nu_1}(\omega) \coth\left(\frac{\omega}{2T_{\nu_1}}\right) [\omega - \Omega(n_2 + n_4 + \mu)] \\ \times \mathcal{J}_2(\omega - \Omega(n_2 + n_4 + \mu)) \tilde{G}_\mu(-\omega + n_4\Omega) \tilde{G}_{-(n_{\text{tot}} + \mu)}(\omega + n_3\Omega). \quad (48)$$

Again, using Eq. (41), and letting $\mu + n_2 + n_4 \rightarrow \mu$, we can rewrite

$$J_2^{(b)} = - \frac{1}{2\pi m^2} \sum_{n_1, n_2=-\infty}^{\infty} g_{n_1,2} g_{n_2,2} \sum_{n_3, n_4=-\infty}^{+\infty} \sum_{\nu_1=1}^2 g_{n_3, \nu_1} g_{n_4, \nu_1} \sum_{\mu=-\infty}^{+\infty} \int_{-\infty}^{+\infty} d\omega \mathcal{J}_{\nu_1}(\omega) \coth\left(\frac{\omega}{2T_{\nu_1}}\right) (\omega - \mu\Omega) \mathcal{J}_2(\omega - \mu\Omega) \\ \times \text{Re} \left[\tilde{G}_{\mu-(n_2+n_4)}(-\omega + n_4\Omega) \tilde{G}_{-(\mu+n_1+n_3)}(\omega + n_3\Omega) \right] \quad (49)$$

Now, recalling that $n_1 = n_2 = 0$ for $\nu = 2$, and performing the sum over $n_3, n_4 = \pm 1$ in the $\nu_1 = 1$ term, we arrive at the final expression

$$J_2 = \frac{1}{2\pi m} \sum_{\mu=-\infty}^{+\infty} \int_{-\infty}^{+\infty} d\omega \left\{ \mathcal{J}_2(\omega) \coth\left(\frac{\omega}{2T_2}\right) \left[\omega \text{Im} \left[\tilde{G}_0(\omega) \right] \delta_{\mu,0} - \frac{\mathcal{J}_2(\omega - \mu\Omega)}{m} (\omega - \mu\Omega) \left| \tilde{G}_\mu(\omega) \right|^2 \right] + \right. \\ \left. - \frac{\mathcal{J}_1(\omega)}{4m^2} \coth\left(\frac{\omega}{2T_1}\right) (\omega - \mu\Omega) \mathcal{J}_2(\omega - \mu\Omega) \left| \tilde{G}_{\mu-1}(-\omega + \Omega) + \tilde{G}_{\mu+1}(-\omega - \Omega) \right|^2 \right\}. \quad (50)$$

A useful property of the Floquet coefficients

Here we prove that, for the dynamical couplings considered in this work, the property in Eq. (42) holds true. In particular, for a generic bath on contact 1 with $\tilde{\gamma}_1(\omega) = \gamma_1\phi(\omega)$, Eq. (14) can be conveniently rewritten as

$$\tilde{G}_\mu(\omega) = D_0(\omega)\delta_{\mu,0} + \lambda D_\mu(\omega) \left[J_{\mu,\mu-2}(\omega)\tilde{G}_{\mu-2}(\omega) + J_{\mu,\mu+2}(\omega)\tilde{G}_{\mu+2}(\omega) \right], \quad (51)$$

where we have introduced

$$\lambda = \frac{\gamma_1}{\omega_0}; \quad D_\mu(\omega) = \chi(\omega + \mu\Omega); \quad J_{\mu,\mu'}(\omega) = \frac{i\omega_0}{4} \left(\omega + \frac{\mu + \mu'}{2}\Omega \right) \phi \left(\omega + \frac{\mu + \mu'}{2}\Omega \right). \quad (52)$$

We now write a formal series expansion of $\tilde{G}_\mu(\omega)$ in powers of λ :

$$\tilde{G}_\mu(\omega) = \sum_{n \geq 0} \lambda^n \tilde{G}_\mu^{(n)}(\omega), \quad (53)$$

which is plugged into Eq. (51). Matching order-by-order in λ a hierarchy of nested equations for the n -th contribution $\tilde{G}_\mu^{(n)}(\omega)$ is obtained. In particular one immediately sees that $\tilde{G}_0^{(0)}(\omega) = D_0(\omega)$ and that

$$\tilde{G}_\mu^{(n+1)}(\omega) = D_\mu(\omega) \left[J_{\mu,\mu-2}(\omega)\tilde{G}_{\mu-2}^{(n)}(\omega) + J_{\mu,\mu+2}(\omega)\tilde{G}_{\mu+2}^{(n)}(\omega) \right]. \quad (54)$$

From Eq. (54) one can conclude that:

(1) $\tilde{G}_{2\mu+1}^{(n)}(\omega) \equiv 0$ for all μ and $n \geq 0$;

(2) For given $n \geq 0$ the only possible nonzero $\tilde{G}_\mu^{(n)}(\omega)$ occur for $|\mu| \leq 2n$ with $\mu \in \{-2n, -2n+4, \dots, 2n-4, 2n\}$.

One can picture the set of $\tilde{G}_\mu^{(n)}(\omega)$ satisfying $n \geq 0$ and $|\mu| \leq 2n$ as a lattice of dots on a Pascal triangle, whose rows are labeled by n and whose columns are labeled by μ . This is represented in Fig. 4, where green (red) dots represent the non-zero (zero) $\tilde{G}_\mu^{(n)}(\omega)$.

Equations (54) can be solved recursively. As an example, to first order one immediately finds $G_{\pm 2}^{(1)}(\omega) = D_{\pm 2}(\omega)J_{\pm 2,0}(\omega)D_0(\omega)$. As another example, a non-trivial solution for the second order is

$$G_0^{(2)}(\omega) = D_0(\omega)J_{0,2}(\omega)D_2(\omega)J_{2,0}(\omega)D_0(\omega) + D_0(\omega)J_{0,-2}(\omega)D_{-2}(\omega)J_{-2,0}(\omega)D_0(\omega). \quad (55)$$

Each term in the above equation can be interpreted as a *path* on the Pascal triangle, linking dots (μ, n) and (μ, n') *within the triangle* according to the simple rule $|\mu - \mu'| = 2$ and $|n - n'| = 1$. To each dot a factor $D_\mu(\omega)$ is associated, to each link between dots a factor $J_{\mu, \mu'}(\omega)$ is associated. Explicitly, the two paths representing the terms in Eq. (55) are $(0, 2) \rightarrow (2, 1) \rightarrow (0, 0)$ and $(0, 2) \rightarrow (-2, 1) \rightarrow (0, 0)$ respectively. Notice that the index n to the l.h.s. of gives the number n of links between the $n+1$ dots.

Proceeding with the recursion one quickly realizes that the situation depicted above is general. Indeed, the term $\tilde{G}_\mu^{(n)}(\omega)$ consists of a sum of $\mathcal{N}(n, \mu) = \binom{n}{\frac{2n-\mu}{4}}$ terms

$$\tilde{G}_\mu^{(n)}(\omega) = \sum_{j=1}^{\mathcal{N}(n, \mu)} \tilde{G}_\mu^{(n, j)}(\omega), \quad (56)$$

where $\tilde{G}_\mu^{(n, j)}(\omega)$ is associated to one of *all* the $\mathcal{N}(n, \mu)$ distinct paths $\mathcal{P}_j(\mu, n)$ (with $1 \leq j \leq \mathcal{N}(n, \mu)$) that connect the dot (μ, n) with $(0, 0)$ with n links that follow the rules $|\mu - \mu'| = 2$ and $|n - n'| = 1$ as stated above.

More formally, each path $\mathcal{P}_j(\mu, n)$ associated to $\tilde{G}_\mu^{(n, j)}(\omega)$ can be represented by the sequence of dots

$$\mathcal{P}_j(\mu, n) = \{(\mu_n^{(j)}, n), (\mu_{n-1}^{(j)}, n-1), \dots, (\mu_0^{(j)}, 0)\}$$

with "fixed boundaries" $\mu_n^{(j)} \equiv \mu$ and $\mu_0^{(j)} = 0$. One of such path for $\mu = 2$ and $n = 5$ is shown as a blue line in Fig. 4. Then, to construct $\tilde{G}_\mu^{(n, j)}(\omega)$ we associate a term $D_{\mu_\nu}(\omega)$ to each dot in the path and a term $J_{\mu_\nu, \mu_{\nu+1}}(\omega)$ to each link between consecutive dots (with $0 \leq \nu < n$) which leads to

$$\tilde{G}_\mu^{(n, j)}(\omega) = D_{\mu_0^{(j)}}(\omega) \prod_{\nu=0}^{n-1} J_{\mu_\nu^{(j)}, \mu_{\nu+1}^{(j)}}(\omega) D_{\mu_{\nu+1}^{(j)}}(\omega). \quad (57)$$

The set of all paths $\mathcal{P}(\bar{\mu}, n) = \cup_{j=1}^{\mathcal{N}(n, \bar{\mu})} \mathcal{P}_j$ contributing to Eq. (56) lies within a rectangular region of the Pascal triangle (a representative example for the case $\mu = 2$ and $n = 5$ is shown as the yellow region in Fig. 4). It is simple to see that such rectangle has vertices

$$A = (0, 0); \quad B = \left(\frac{\mu + 2n}{2}, \frac{2n + \mu}{4} \right); \quad C = \left(\frac{\mu - 2n}{2}, \frac{2n - \mu}{4} \right); \quad D = (\mu, n). \quad (58)$$

To prove Eq. (42) for the n -th order term we need to shift the argument of $\tilde{G}_\mu^{(n)}(\omega)$. To this end, it is useful to observe that

$$D_\mu(\omega + k\Omega) = D_{\mu+k}(\omega); \quad J_{\mu, \mu'}(\omega + k\Omega) = J_{\mu+k, \mu'+k}(\omega), \quad (59)$$

with k an integer. Geometrically, this means that shifting the argument of $\tilde{G}_\mu^{(n)}(\omega)$ by $k\Omega$ is equivalent to shift all paths [82] that contribute to it (and hence the whole set $\mathcal{P}(\bar{\mu}, n)$) by $|k|\Omega$ to the right or to the left according to $\text{Sgn}(k)$.

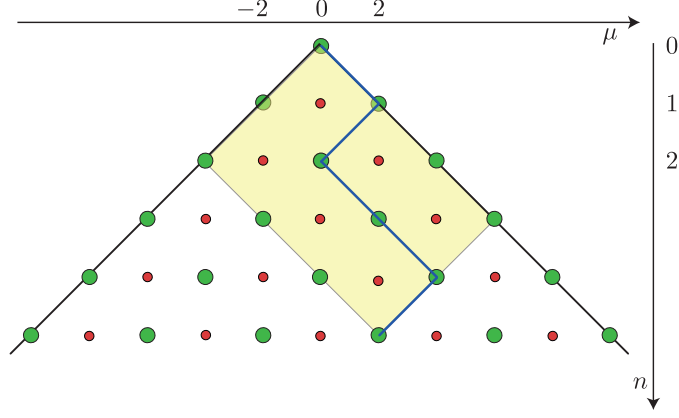


FIG. 4. The Pascal triangle of dots representing the set of all points associated with $\tilde{G}_\mu^{(n)}(\omega)$: Green (red) dots represent a non-zero (zero) $\tilde{G}_\mu^{(n)}(\omega)$. The blue line represents one of the paths contributing to $\tilde{G}_2^{(5)}(\omega)$, the yellow shaded line represent the region which contains all possible distinct paths contributing to $\tilde{G}_2^{(5)}(\omega)$.

According to what discussed above, let us denote with \mathcal{P}_+ the region containing all the paths contributing to $\tilde{G}_\mu^{(n)}(\omega - \frac{\mu}{2}\Omega)$, with vertices

$$A_+ = \left(-\frac{\mu}{2}, 0\right); \quad B_+ = \left(n, \frac{2n + \mu}{4}\right); \quad C_+ = \left(-n, \frac{2n - \mu}{4}\right); \quad D_+ = \left(\frac{\mu}{2}, n\right), \quad (60)$$

while the paths contributing to $\tilde{G}_{-2\mu}^{(n)}(\omega + \mu\Omega)$ belong to the region \mathcal{P}_- with vertices

$$A_- = \left(\frac{\mu}{2}, 0\right); \quad B_- = \left(n, \frac{2n - \mu}{4}\right); \quad C_- = \left(-n, \frac{2n + \mu}{4}\right); \quad D_- = \left(-\frac{\mu}{2}, n\right). \quad (61)$$

Observe that all the factors in Eq. (57) actually depend only on the ordered set $\{\mu_\nu^{(j)}\}$ but are invariant under any permutation of the second coordinate of each lattice point. This allows to re-order the vertices of \mathcal{P}_- in decreasing order of their second coordinate as

$$A_- = \left(\frac{\mu}{2}, n\right) \equiv D_+; \quad B_- = \left(n, \frac{2n + \mu}{4}\right) \equiv B_+; \quad C_- = \left(-n, \frac{2n - \mu}{4}\right) \equiv C_+; \quad D_- = \left(-\frac{\mu}{2}, 0\right) \equiv A_+. \quad (62)$$

This allows us to conclude that the two regions are actually identical. Since shifting the argument only amounts to a rigid translation of the paths and the actual re-ordering performed above corresponds to reading each term from right to left rather than left to right, it follows that to each path of $\tilde{G}_\mu^{(n)}(\omega - \frac{\mu}{2}\Omega)$ identically corresponds one and only one term of $\tilde{G}_{-\mu}^{(n)}(\omega + \frac{\mu}{2}\Omega)$. This allows to conclude that $\tilde{G}_\mu^{(n)}(\omega - \frac{\mu}{2}\Omega) = \tilde{G}_{-\mu}^{(n)}(\omega + \frac{\mu}{2}\Omega)$ is valid $\forall n$. By virtue of the series expansion in Eq. (53), the above property is valid also for the complete $\tilde{G}_\mu(\omega)$:

$$\tilde{G}_\mu\left(\omega - \frac{\mu}{2}\Omega\right) = \tilde{G}_{-\mu}\left(\omega + \frac{\mu}{2}\Omega\right).$$

Weak coupling

In this section we derive closed expressions for the average power and heat currents in the weak coupling, perturbative regime – i.e. assuming $|\mathcal{J}_1(\omega)| \ll |\mathcal{J}_2(\omega)|$. The starting point are the general forms previously obtained for the power in Eqs. (43), (45), (46) and for the heat current in Eq. (50). We first need the perturbative expansion of the Floquet coefficients in Eq. (14), which, recalling Eq. (38), can be written up to linear order in \mathcal{J}_1 as

$$\begin{aligned} \tilde{G}_0(\omega) &= \chi_0(\omega) \left[1 + \frac{i}{4} [\omega_+ \tilde{\gamma}_1(\omega_+) + \omega_- \tilde{\gamma}_1(\omega_-)] \chi_0(\omega) \right], \\ \tilde{G}_{\pm 2}(\omega) &= \frac{i}{4} \chi_0(\omega \pm 2\Omega) \omega_\pm \tilde{\gamma}_1(\omega_\pm) \chi_0(\omega), \\ \tilde{G}_{|m|>2} &= \mathcal{O}(\mathcal{J}_1^2). \end{aligned} \quad (63)$$

Above we have introduced the bare susceptibility

$$\chi_0(\omega) = -\frac{1}{\omega^2 - \omega_0^2 + i\omega\tilde{\gamma}_2(\omega)}, \quad (64)$$

with effective damping $\tilde{\gamma}_2(\omega)$. Notice that this quantity fulfill the relation

$$\text{Im}[\chi_0(\omega)] = \omega|\chi_0(\omega)|^2 \text{Re}[\tilde{\gamma}_2(\omega)] = \frac{1}{m}\mathcal{J}_2(\omega)|\chi_0(\omega)|^2. \quad (65)$$

Considering the average power, we should evaluate Eqs. (43), (45) and (46) up to linear order in \mathcal{J}_1 . The first contribution is already linear in \mathcal{J}_1 , hence, by using the zero-th term $\tilde{G}_0(\omega) = \chi_0(\omega)$ in Eq. (63) one has

$$P^{(a)} = -\frac{\Omega}{4\pi m} \int_{-\infty}^{+\infty} d\omega \mathcal{J}_1(\omega) \coth\left(\frac{\omega}{2T_1}\right) \text{Im}[\chi_0(\omega - \Omega)]. \quad (66)$$

Eq. (45) does not contribute, since it starts at second order in \mathcal{J}_1 ; using Eq. (65) we can write the first order contribution of Eq. (46) as

$$P^{(b,2)} = \frac{\Omega}{8\pi m} \int_{-\infty}^{+\infty} d\omega \coth\left(\frac{\omega}{2T_2}\right) \text{Im}[\chi_0(\omega)] [\mathcal{J}_1(\omega + \Omega) - \mathcal{J}_1(\omega - \Omega)]. \quad (67)$$

Combining the above expressions, the total power reads

$$P = -\Omega \int_{-\infty}^{+\infty} \frac{d\omega}{4\pi m} \mathcal{J}_1(\omega + \Omega) \text{Im}[\chi_0(\omega)] \left[\coth\left(\frac{\omega + \Omega}{2T_1}\right) - \coth\left(\frac{\omega}{2T_2}\right) \right]. \quad (68)$$

Finally, using $\coth(x/2) = 1 + 2n_B(x)$ with $n_B(x) = (e^x - 1)^{-1}$ the Bose distribution function, we arrive at

$$P = -\Omega \int_0^{+\infty} \frac{d\omega}{4\pi m} \text{Im} \chi_0(\omega) \left[\mathcal{J}_1(\omega_+) n_B\left(\frac{\omega_+}{T_1}\right) - \mathcal{J}_1(\omega_-) n_B\left(\frac{\omega_-}{T_1}\right) + [\mathcal{J}_1(\omega_-) - \mathcal{J}_1(\omega_+)] n_B\left(\frac{\omega}{T_2}\right) \right]. \quad (69)$$

We now focus on the average current J_2 as reported in Eq. (50). To this end, we can use the following relations (valid up to linear order in \mathcal{J}_1):

$$|\tilde{G}_0(\omega)|^2 = |\chi_0(\omega)|^2 \left[1 - \frac{1}{2} \sum_{p=\pm} \omega_p \text{Im} \left(\chi_0(\omega) \tilde{\gamma}_1(\omega_p) \right) \right] \quad (70)$$

and

$$\text{Im} \tilde{G}_0(\omega) = \text{Im} \chi_0(\omega) + \frac{1}{4} \sum_{p=\pm} \omega_p \left[\text{Re} \left(\chi_0(\omega) \right) \text{Re} \left(\chi_0(\omega) \tilde{\gamma}_1(\omega_p) \right) - \text{Im} \left(\chi_0(\omega) \right) \text{Im} \left(\chi_0(\omega) \tilde{\gamma}_1(\omega_p) \right) \right]. \quad (71)$$

Comparing the two above equations and remembering that $\text{Im} \chi_0(\omega) = \frac{1}{m} \mathcal{J}_2(\omega) |\chi_0(\omega)|^2$ we can write

$$\frac{\mathcal{J}_2(\omega)}{m} |\tilde{G}_0(\omega)|^2 = \text{Im} \tilde{G}_0(\omega) - \frac{1}{4m} |\chi_0(\omega)|^2 \sum_{p=\pm} \mathcal{J}_1(\omega_p). \quad (72)$$

Plugging these expressions into Eq. (50) and using the explicit form of $\tilde{G}_{\pm 2}(\omega)$ in Eq. (63) (linear in \mathcal{J}_1) we arrive at the compact form

$$J_1 = \int_{-\infty}^{+\infty} \frac{d\omega}{4\pi m} (\omega + \Omega) \mathcal{J}_1(\omega + \Omega) \text{Im} \chi_0(\omega) \left[\coth\left(\frac{\omega + \Omega}{2T_1}\right) - \coth\left(\frac{\omega}{2T_2}\right) \right], \quad (73)$$

$$J_2 = - \int_{-\infty}^{+\infty} \frac{d\omega}{4\pi m} \omega \mathcal{J}_1(\omega + \Omega) \text{Im} \chi_0(\omega) \left[\coth\left(\frac{\omega + \Omega}{2T_1}\right) - \coth\left(\frac{\omega}{2T_2}\right) \right], \quad (74)$$

where for sake of completeness we have quoted also the expression for J_1 that can be derived via $J_1 = -(P + J_2)$.

Paradigmatic examples in the weak coupling regime

Here we discuss in more details the paradigmatic examples presented in the main text, where we focused on the case of a Ohmic bath for the static contact 2, with $\tilde{\gamma}_2(\omega) = \gamma_2 \ll \omega_0$. In this regime the bare susceptibility is well described by

$$\text{Im}\{\chi_0(\omega)\} \approx \frac{\pi}{2\omega_0} [\delta(\omega - \omega_0) - \delta(\omega + \omega_0)] . \quad (75)$$

Plugging Eq. (75) into Eqs. (69), (73) and (74) we obtain the average power and heat currents

$$P = -\frac{\Omega}{4m\omega_0} \sum_{p=\pm 1} p \mathcal{J}_1(\omega_0 + p\Omega) \left[n_B \left(\frac{\omega_0 + p\Omega}{T_1} \right) - n_B \left(\frac{\omega_0}{T_2} \right) \right] , \quad (76)$$

$$J_1 = \frac{1}{4m} \sum_{p=\pm 1} \left(\frac{\omega_0 + p\Omega}{\omega_0} \right) \mathcal{J}_1(\omega_0 + p\Omega) \left[n_B \left(\frac{\omega_0 + p\Omega}{T_1} \right) - n_B \left(\frac{\omega_0}{T_2} \right) \right] , \quad (77)$$

$$J_2 = -\frac{1}{4m} \sum_{p=\pm 1} \mathcal{J}_1(\omega_0 + p\Omega) \left[n_B \left(\frac{\omega_0 + p\Omega}{T_1} \right) - n_B \left(\frac{\omega_0}{T_2} \right) \right] . \quad (78)$$

In the following, we will focus on the $\Omega > 0$ regime.

No heat engine for Ohmic and sub-Ohmic spectral function

Here we show that when $\mathcal{J}_1(\omega) = m\gamma_1\omega \left| \frac{\omega}{\omega_0} \right|^{s-1}$ and $0 < s \leq 1$ no working heat engine can be achieved. Note that in this section we assume that the cut-off ω_c is the largest energy scale ($\omega_c \gg \omega_0, \Omega$). We start observing that given Eq. (75) the condition of Eq. (11) in the main text becomes $f(\omega_0, \Omega) > 0$. The best-case scenario for this monotonic spectral density occurs when $T_2 \rightarrow 0$, as also discussed in the main text, since it minimizes for given s, Ω, T_1 the positive contribution $\propto [\mathcal{J}_1(\omega_0 + \Omega) - \mathcal{J}_1(\omega_0 - \Omega)] n_B \left(\frac{\omega_0}{T_2} \right)$ to the power P and thus maximizes the power output. The condition $f(\omega_0, \Omega) > 0$ is then equivalent to

$$(\omega_0 + \Omega) |\omega_0 + \Omega|^{s-1} n_B \left(\frac{\omega_0 + \Omega}{T_1} \right) > (\omega_0 - \Omega) |\omega_0 - \Omega|^{s-1} n_B \left(\frac{\omega_0 - \Omega}{T_1} \right) . \quad (79)$$

Observing that $(\omega_0 - \Omega) n_B \left(\frac{\omega_0 - \Omega}{T_1} \right) > 0$ always, with a simple rearrangement the above equation becomes

$$f_s(\Omega) > g_{T_1}(\Omega) \quad (80)$$

where

$$f_s(\Omega) = \left| \frac{\omega_0 + \Omega}{\omega_0 - \Omega} \right|^s \quad (81)$$

$$g_{T_1}(\Omega) = \left| \frac{n_B((\omega_0 - \Omega)/T_1)}{n_B((\omega_0 + \Omega)/T_1)} \right| . \quad (82)$$

We firstly observe that both $f_s(\Omega)$ and $g_{T_1}(\omega)$ are continuous functions of Ω except at $\Omega = \omega_0$ where they diverge as

$$f_s(\Omega) \approx \frac{(2\omega_0)^s}{|\omega_0 - \Omega|^s} \quad ; \quad g_{T_1}(\Omega) \approx \frac{T_1 (e^{2\omega_0/T_1} - 1)}{|\omega_0 - \Omega|} \quad \text{when } \Omega \rightarrow \omega_0 . \quad (83)$$

At least for $\Omega \approx \omega_0$ and $0 < s \leq 1$ it is then clear that $f_s(\Omega) < g_{T_1}(\Omega)$ and thus no working engine can be obtained there. To prove that this is the case for any Ω we now inspect the general properties of $f_s(\Omega)$ and $g_{T_1}(\Omega)$, and their derivatives, to show that for $0 < s \leq 1$ Eq. (80) cannot be verified. Observe that

$$\frac{df_s(\Omega)}{d\Omega} = s \left(\frac{2\omega_0}{\omega_0^2 - \Omega^2} \right) f_s(\Omega) \quad \text{for } \Omega \neq \omega_0 , \quad (84)$$

and

$$\frac{dg_{T_1}(\Omega)}{d\Omega} = \phi_{T_1}(\Omega)g_{T_1}(\Omega), \quad (85)$$

where

$$\phi_{T_1}(\Omega) = \begin{cases} \frac{1+\delta_{T_1}(\Omega)}{T_1} & \text{if } 0 < \Omega < \omega_0 \\ \frac{\delta_{T_1}(\Omega)}{T_1} & \text{if } \Omega > \omega_0 \end{cases} \quad (86)$$

with $\delta_{T_1}(\Omega) = \sinh(\omega_0/T_1)/[\cosh(\omega_0/T_1) - \cosh(\Omega/T_1)]$. It can be checked (not shown here) that $\phi_{T_1}(\Omega)$ is a monotonically decreasing function of T_1 and that

$$\lim_{T_1 \rightarrow \infty} \phi_{T_1}(\Omega) = \frac{2\omega_0}{\omega_0^2 - \Omega^2} = \frac{1}{sf_s(\Omega)} \frac{df_s(\Omega)}{d\Omega}, \quad (87)$$

where in the second passage we have used Eq. (84). Thus we arrive at the following inequality

$$\frac{dg_{T_1}(\Omega)}{d\Omega} > \frac{1}{s} \frac{g_{T_1}(\Omega)}{f_s(\Omega)} \frac{df_s(\Omega)}{d\Omega}. \quad (88)$$

Integrating Eq. (88) from 0 to Ω one obtains $f_s(\Omega) < g_{T_1}^s(\Omega)$ or equivalently

$$\frac{f_s(\Omega)}{g_{T_1}(\omega)} < g_{T_1}^{s-1}(\Omega). \quad (89)$$

Since $g_{T_1}(\Omega) > 1$ for $\Omega > 0$, from the last inequality it follows that if $0 < s \leq 1$ one has $f_s(\Omega) < g_{T_1}(\Omega)$. This is in contrast with Eq. (80) and this shows that no engine can be achieved for $0 < s \leq 1$.

Efficiency of a super-Ohmic engine

Here we analyze the efficiency $\eta = -P/J_1$ (for $P < 0$) of a super-Ohmic engine. In Sec. we have commented that, for given s, Ω, T_1 the limit $T_2 \rightarrow 0$ maximizes the power output of the engine. Indeed, it can also be proven (not shown here) that for given s, Ω, T_1 the efficiency η is a *decreasing* function of T_2 and thus that considering the limit $T_2 \rightarrow 0$ is the best case scenario also for the efficiency [83]. In this limit, from Eqs. (76), (77) the efficiency $\eta(s, T_1, \Omega)$ reads

$$\eta(s, T_1, \Omega) = \Omega \frac{(\omega_0 + \Omega)^s n_B \left(\frac{\omega_0 + \Omega}{T_1} \right) - |\omega_0 - \Omega|^s \left| n_B \left(\frac{\omega_0 - \Omega}{T_1} \right) \right|}{(\omega_0 + \Omega)^{s+1} n_B \left(\frac{\omega_0 + \Omega}{T_1} \right) + (\omega_0 - \Omega) |\omega_0 - \Omega|^s \left| n_B \left(\frac{\omega_0 - \Omega}{T_1} \right) \right|}. \quad (90)$$

From the above equation one immediately finds

$$\lim_{\Omega \rightarrow \omega_0} \eta(s, T_1, \Omega) = \frac{1}{2} \quad \forall s, T_1. \quad (91)$$

Let us now study the efficiency for $\Omega \neq \omega_0$, which can also be written as

$$\eta(s, T_1, \Omega) = \frac{\Omega}{|\omega - \Omega|} \frac{f_s(\Omega) - g_{T_1}(\Omega)}{f_{s+1}(\Omega) + g_{T_1}(\Omega) \text{Sgn}(\omega - \Omega)}, \quad (92)$$

recalling the definitions of Eqs. (81), (82). Furthermore,

$$\frac{\partial \eta(s, T_1, \Omega)}{\partial T_1} = -g'_{T_1}(\Omega) \frac{\Omega}{|\omega_0 - \Omega|} \frac{f_{s+1}(\Omega) + f_s(\Omega) \text{Sgn}(\omega_0 - \Omega)}{[f_{s+1}(\Omega) + g_{T_1}(\Omega) \text{Sgn}(\omega_0 - \Omega)]^2} > 0 \quad (93)$$

since

$$g'_{T_1} = \frac{\partial g_{T_1}(\Omega)}{\partial T_1} < 0 \quad \text{for } \Omega > 0, \quad (94)$$

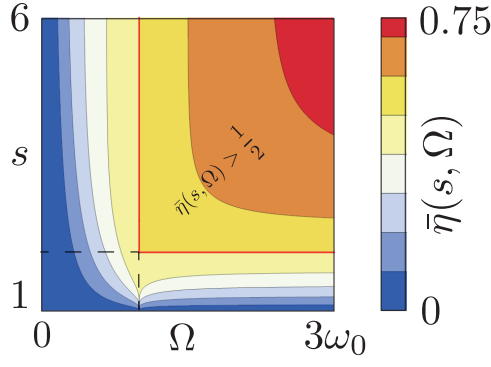


FIG. 5. Contour plot of $\bar{\eta}(s, \Omega)$ as a function of Ω and s . Contour lines spacing is 0.1, the contour at $\bar{\eta}(s, \Omega) = 0.5$ is shown with red lines for reference. The horizontal dashed line marks the value $s = 2$, the vertical dashed line marks $\Omega = \omega_0$.

as can be proven by direct calculation and $f_s(\Omega)$ is an increasing function of s . It follows that $\eta(s, T_1, \Omega)$ is a monotonically increasing function of T_1 , with an upper bound $\bar{\eta}(s, \Omega)$ given by

$$\bar{\eta}(s, \Omega) = \lim_{T_1 \rightarrow \infty} \eta(s, T_1, \Omega) = \frac{\Omega}{|\omega_0 - \Omega|} \frac{f_{s-1}(\Omega) - 1}{f_s(\Omega) + \text{Sgn}(\omega_0 - \Omega)}. \quad (95)$$

A contour plot of $\bar{\eta}(s, \Omega)$ is shown in Fig. (5), which clearly shows that for $1 < s \leq 2$ one has always $\bar{\eta}(s, \Omega) \leq 1/2$ (and thus $\eta(s, T_1, \Omega) \leq 1/2$), while for $s > 2$ it is possible to achieve $\eta(s, \Omega, T_1) > 1/2$ for $\Omega > \omega_0$ and large enough temperature.

Engine for a Ohmic bath with a hard cutoff

In this section we study the case of a Ohmic bath with a finite cutoff ω_c

$$\mathcal{J}_1(\omega) = m\gamma_1\omega\theta(\omega_c - |\omega|). \quad (96)$$

The presence of a step-like cut-off modifies the strictly Ohmic spectral function and introduces non-Markovian effects.

The average power in Eq. (76) now reads

$$P = -\frac{\gamma_1\Omega}{4\omega_0} \sum_{p=\pm 1} p(\omega_0 + p\Omega)\theta(\omega_c - |\omega_0 + p\Omega|) \left[n_B\left(\frac{\omega_0 + p\Omega}{T_1}\right) - n_B\left(\frac{\omega_0}{T_2}\right) \right]. \quad (97)$$

We first consider the case $0 < \omega_c < \omega_0$. In this case $\omega_c < \omega_0 + \Omega$ and to achieve $P < 0$ one needs $\omega_c > |\omega_0 - \Omega|$. The average power then reads

$$P = -\frac{\gamma_1\Omega}{4\omega_0}(\omega_0 - \Omega) \left[n_B\left(\frac{\omega_0}{T_2}\right) - n_B\left(\frac{\omega_0 - \Omega}{T_1}\right) \right]. \quad (98)$$

Clearly, for $\Omega > \omega_0$ one has $P > 0$, while for $\omega_0 - \omega_c < \Omega < \omega_0$ the condition $P < 0$ implies

$$n_B\left(\frac{\omega_0}{T_2}\right) > n_B\left(\frac{\omega_0 - \Omega}{T_1}\right), \quad (99)$$

which yields the condition

$$T_2 > T_1 \frac{\omega_0}{\omega_0 - \Omega} \quad \text{or equivalently} \quad \Omega < \omega_0 \left(1 - \frac{T_1}{T_2}\right). \quad (100)$$

The positive average heat current is J_2 , given by

$$J_2 = \frac{\gamma_1}{4}(\omega_0 - \Omega) \left[n_B\left(\frac{\omega_0}{T_2}\right) - n_B\left(\frac{\omega_0 - \Omega}{T_1}\right) \right], \quad (101)$$

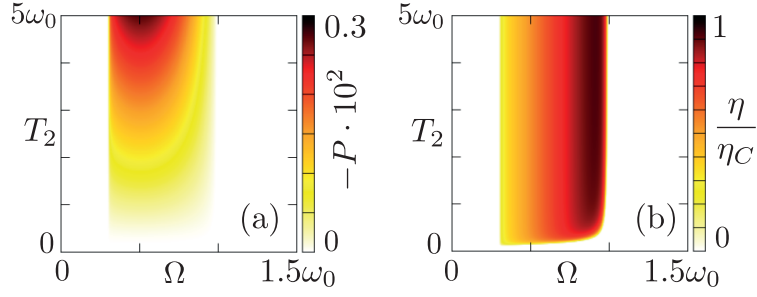


FIG. 6. Density plot of (a) the power $-P$ (in unit of γ_2^2) and (b) the normalized efficiency η/η_C for a Ohmic spectral density with hard cutoff, as a function of the driving frequency Ω and T_1 (in units of ω_0). In all panels $\gamma_1 = 10^{-2}\gamma_2$, $\gamma_2 = 10^{-2}\omega_0$, $T_1 = 10^{-2}\omega_0$ and $\omega_c = 0.7\omega_0$.

so that the efficiency is $\eta = -P/J_2 = \Omega/\omega_0$. From the condition in Eq. (100) it is clear that $\eta \leq \eta_C = 1 - \frac{T_1}{T_2}$, with $P \rightarrow 0$ when $\eta \rightarrow \eta_C$.

When $\omega_c \geq \omega_0$, to obtain $P < 0$ one needs $\omega_c - \omega_0 < \Omega < \omega_c + \omega_0$ [84]. Note however that also in this case the power is still given by Eq. (98). This in particular implies that to have $P < 0$ one must further restrict the drive frequency to $\omega_c - \omega_0 < \Omega < \omega_0$, which ultimately implies $\omega_c < 2\omega_0$. Also in this case the conditions at Eq. (100) must hold, the efficiency is still given by $\eta\Omega/\omega_0$ with $\eta \leq \eta_C$ and $P \rightarrow 0$ when $\eta \rightarrow \eta_C$.

To support the analytic approach presented above, we show in Fig. (6) the power and efficiency obtained numerically evaluating Eqs. (69) and (74) with $\mathcal{J}_1(\omega)$ given in Eq. (96) for $\omega_c = 0.7\omega_0$. All the features are in excellent agreement with the analytic calculations shown previously.

Maximum efficiency in the Lorentzian case

Here, we discuss engine performance in the case of a Lorentzian structured spectral density of the form

$$\mathcal{J}_1(\omega) = d_1 \frac{m\gamma_1\omega}{(\omega^2 - \omega_1^2)^2 + \gamma_1^2\omega^2}. \quad (102)$$

The coupling strength is controlled by the dimensionless parameter

$$\kappa = \frac{d_1}{\omega_0^2\omega_1^2}. \quad (103)$$

Here we focus on the weak coupling regime $\kappa \ll 1$ with $\gamma_1 \ll \text{Min}[\omega_0, \omega_1]$, consistently with the discussion in the main text. This corresponds to a sharp Lorentzian peaked at ω_1 and from Eq. (76) it is clear that the best-case scenario is represented by the resonance condition $\omega_1 = \omega_0 \pm \Omega$. For $\omega_1 = \omega_0 + \Omega$ one has $\mathcal{J}_1(\omega_1) \gg \mathcal{J}_1(\omega_0 - \Omega)$, while for $\omega_1 = \omega_0 - \Omega$ one has $\mathcal{J}_1(\omega_1) \gg \mathcal{J}_1(\omega_0 + \Omega)$. To derive useful analytical expressions, we only retain terms $\propto \mathcal{J}_1(\omega_1)$ in Eqs. (76), (78). It then follows that to have $P < 0$

- for $\omega_1 = \omega_0 + \Omega$, one needs $n_B\left(\frac{\omega_1}{T_1}\right) > n_B\left(\frac{\omega_0}{T_2}\right)$, which implies $\omega_1 < \frac{T_1}{T_2}\omega_0$. Since on the other hand $\omega_1 > \omega_0$ in this case, the above condition implies $T_2 < T_1$ and the conditions can be summarized as

$$\text{Engine condition for } \omega_1 = \omega_0 + \Omega: \quad \omega_0 < \omega_1 < \frac{T_1}{T_2}\omega_0 \quad \text{with} \quad T_2 < T_1,$$

while on the other hand

- for $\omega_1 = \omega_0 - \Omega$ it is required that $n_B\left(\frac{\omega_1}{T_1}\right) < n_B\left(\frac{\omega_0}{T_2}\right)$, which implies $\omega_1 > \frac{T_1}{T_2}\omega_0$. Since in this case $\omega_1 < \omega_0$ one must have $T_1 < T_2$ in this case and we can summarize the

$$\text{Engine condition for } \omega_1 = \omega_0 - \Omega: \quad \frac{T_1}{T_2}\omega_0 < \omega_1 < \omega_0 \quad \text{with} \quad T_1 < T_2.$$

In both cases, it is also simple to obtain the efficiency of the Lorentzian engine from Eqs. (76)-(78):

$$\text{the engine efficiency for } \omega_1 = \omega_0 + \Omega \text{ is } \eta = \frac{\Omega}{\omega_1} = 1 - \frac{\omega_0}{\omega_1},$$

while

$$\text{the engine efficiency for } \omega_1 = \omega_0 - \Omega \text{ is } \eta = \frac{\Omega}{\omega_0} = 1 - \frac{\omega_1}{\omega_0}.$$

Recalling the conditions to obtain a Lorentzian engine discussed above, the two expressions can be combined as

$$\eta = 1 - \frac{\text{Min}[\omega_0, \omega_1]}{\text{Max}[\omega_0, \omega_1]}. \quad (104)$$

In both cases, it is immediately visible that the maximum efficiency is the Carnot efficiency

$$\eta_C = 1 - \frac{\text{Min}[T_1, T_2]}{\text{Max}[T_1, T_2]}, \quad (105)$$

and that when $\eta \rightarrow \eta_C$ then $P \rightarrow 0$.

Beyond weak coupling

Average power in the Markovian regime beyond weak coupling

In this part we demonstrate that a bath modulated in time with a Markovian dynamics will never support a heat engine at any order in the system/bath interaction. We start by selecting for the modulated bath ($\nu = 1$) the spectral function which can induce a Markovian dynamics on the QHO. We remind that a Markovian regime corresponds to a bath kernel $\langle \xi_1(t)\xi_1(t') \rangle = \mathcal{L}_1(t-t') \propto \delta(t-t')$, with a constant Fourier transform $\tilde{\mathcal{L}}_1(\omega)$. From (12), we have

$$\tilde{\mathcal{L}}_1(\omega) = \mathcal{J}_1(\omega) \left[\coth\left(\frac{\omega}{2T_1}\right) + 1 \right]. \quad (106)$$

Then in order to have $\tilde{\mathcal{L}}_1(\omega) = \text{constant}$ we need to chose a Ohmic spectral function

$$\mathcal{J}_1(\omega) = m\gamma_1\omega, \quad (107)$$

which at high temperatures $T \gg \omega$ describes the Markovian regime with $\tilde{\mathcal{L}}_1(\omega) = 2m\gamma_1T_1$. Note that we consider the so-called strictly Ohmic case, with the cut-off $\omega_c \rightarrow \infty$ that well describes all the realistic cases when ω_c is the highest characteristic energy scale [28]. On the other hand, we will not assume any particular shape for the $\mathcal{J}_2(\omega)$.

We insert $\mathcal{J}_1(\omega)$ into Eqs. (43), (45) and (46) to obtain an explicit expression for the average power $P = P^{(a)} + P^{(b,1)} + P^{(b,2)}$. We have

$$P^{(a)} = -\frac{\Omega\gamma_1}{4\pi} \int_{-\infty}^{+\infty} d\omega \omega \coth\left(\frac{\omega}{2T_1}\right) \text{Im} \left[\tilde{G}_0(\omega - \Omega) \right], \quad (108)$$

$$P^{(b,1)} = \frac{\Omega\gamma_1^2}{16\pi} \int_{-\infty}^{+\infty} d\omega \omega \coth\left(\frac{\omega}{2T_1}\right) \sum_{\mu=-\infty}^{+\infty} (\omega - \mu\Omega) |\tilde{G}_\mu(-\omega + \Omega) + \tilde{G}_{\mu+2}(-\omega - \Omega)|^2, \quad (109)$$

and

$$P^{(b,2)} = \frac{\Omega^2\gamma_1}{4\pi m} \int_{-\infty}^{+\infty} d\omega \mathcal{J}_2(\omega) \coth\left(\frac{\omega}{2T_2}\right) \sum_{\mu=-\infty}^{+\infty} |\tilde{G}_\mu(\omega)|^2. \quad (110)$$

It is now easy to see that $P^{(b,2)} \geq 0$. Furthermore, it is possible to show that also $P^{(b,1)} \geq 0$. To do this, by using Eq. (41), we first note that

$$\int_{-\infty}^{+\infty} d\omega \omega \coth\left(\frac{\omega}{2T_1}\right) \sum_{\mu=-\infty}^{+\infty} \omega |\tilde{G}_\mu(-\omega + \Omega) + \tilde{G}_{\mu+2}(-\omega - \Omega)|^2 = 0. \quad (111)$$

Therefore, $P^{(b,1)}$ can be rewritten as

$$P^{(b,1)} = -\frac{\Omega^2 \gamma_1^2}{16\pi} \int_{-\infty}^{+\infty} d\omega \omega \coth\left(\frac{\omega}{2T_1}\right) \sum_{\mu=-\infty}^{+\infty} \mu |\tilde{G}_\mu(-\omega + \Omega) + \tilde{G}_{\mu+2}(-\omega - \Omega)|^2, \quad (112)$$

which after some algebra becomes

$$P^{(b,1)} = \frac{\Omega^2 \gamma_1^2}{16\pi} \int_{-\infty}^{+\infty} d\omega \omega \coth\left(\frac{\omega}{2T_1}\right) \sum_{\mu=-\infty}^{+\infty} |\tilde{G}_\mu(-\omega + \Omega) + \tilde{G}_{\mu+2}(-\omega - \Omega)|^2, \quad (113)$$

manifestly positive. We have thus demonstrated that the total power is

$$P = P^{(a)} + \mathcal{P}, \quad \text{with} \quad \mathcal{P} \equiv P^{(b,1)} + P^{(b,2)} \geq 0. \quad (114)$$

The possibility to have a heat engine will then depend only on the sign of the first term $P^{(a)}$. Let us now consider the Markovian limit of the modulated bath, which as explained above is represented by the Ohmic spectral function at large temperatures $T_1 \rightarrow \infty$. Here, the term $\coth\left(\frac{\omega}{2T_1}\right) \rightarrow \frac{2T_1}{\omega}$ and therefore using the odd parity property of $\text{Im}[\tilde{G}_0(\omega)]$ we have

$$P_1^{(a)} = 0. \quad (115)$$

This finally proves that the average power $P > 0$ in the Markovian regime to all order in the system/bath coupling strength, demonstrating that in this case it is *not* possible to obtain a working heat engine ($P < 0$).

Lorentzian spectral density

To illustrate the case of a heat engine and its performances beyond weak coupling, we study again the Lorentzian structured spectral density of Eq. (102) and proceed numerically by solving Eq. (14) and evaluating the expressions for average power and currents in Eqs. (35), (36) from very weak to strong coupling $0 < \kappa \leq 10$ with κ given in Eq. (103). To obtain the results shown below, a set of Floquet states with $|\mu| \leq 150$ has been adopted as it proved to be adequate to achieve a relative accuracy of 10^{-3} or better in all results [85]. Figure 7 shows results for the average power and the efficiency η/η_C for some representative situations. We start (top row) comparing the weak coupling case shown in Fig.3(c,e) of the main text – where $\kappa = 10^{-3}$ – with the results obtained here for $\kappa = 0.1$: a clear broadening of the power resonance line can be observed (panel a), with the appearance of additional structures (see e.g. around $\Omega \sim \omega_1 = 0.5\omega_0$). The dashed line in panel (a) reveals that the maximum power is no longer achieved along the "bare" resonance $\omega_1 = \omega_0 - \Omega$ but now appears detuned. Also the efficiency normalized to the Carnot limit – see Fig. 7(b) – displays an overall broadening and the occurrence of additional features, occurring around the above mentioned frequencies, in contrast to the weak coupling case.

To further investigate the strong-coupling regime we show in the bottom row the average power (panel c) and efficiency η/η_C (panel d) as a function of the coupling parameter κ and the driving frequency Ω for $\omega_1 = 0.4\omega_0$, near the maximum of Fig. 7(a).

As can be seen, operating the engine beyond weak coupling allows to achieve sensibly larger power outputs. In particular, the maximum power shown in Fig. 7(c) occurs at moderate coupling $\kappa \approx 0.2$ and is almost 6 times larger than the maximum power obtained at weak coupling $\kappa = 10^{-3}$. Generally speaking, the average power is a non-monotonic function of κ and we have observed that for $\kappa \gtrsim 1$ the heat engine is lost, also for every other parameter choice we have tested (not shown here). Furthermore, we notice the presence of additional features in the power plot not present for weak coupling (see the region with $\Omega < 0.2\omega_0$ and $\kappa \gtrsim 0.1$) where the engine power output attains relative (but not absolute) maxima. Looking at the efficiency reported in Fig. 7(d), we find that the maximum efficiency is achieved operating the engine in the weak coupling regime $\kappa \ll 1$. Therefore, the parameter κ is an important factor discriminating whether the engine is needed to operate at maximum efficiency (at the expenses of the power output) or if maximum power out is needed (at the expenses of efficiency).

Before closing, we notice that at stronger coupling strength, a marked detuning of the resonance condition – see Fig. 7(c). Inspecting Eqs. (14), (35), and (36) we notice that all Floquet coefficients contain as a leading term the

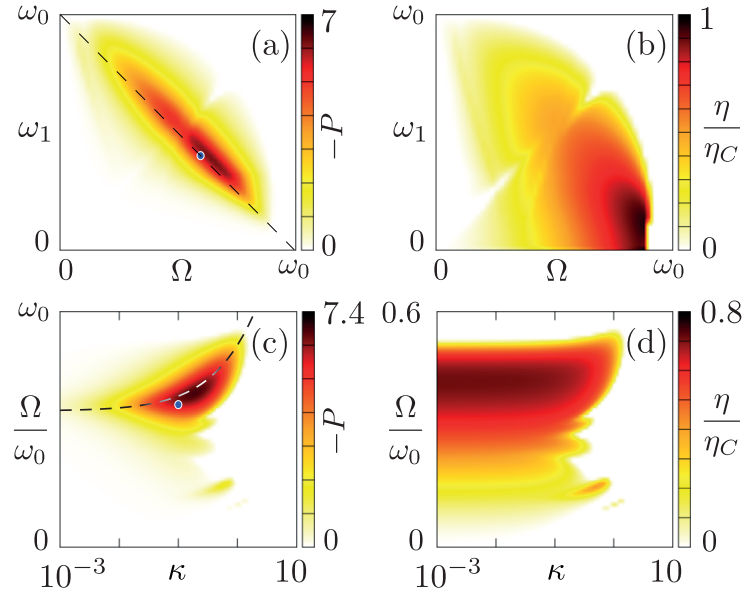


FIG. 7. Heat engine with the Lorentzian structured spectral density of Eq. (102). Top: (a) engine average power (in units of γ_2^2) and (b) efficiency normalized to the Carnot limit η_C as a function of Ω and ω_1 for $\kappa = 0.1$, $T_1 = 0.2\omega_0$ and $T_2 = 2\omega_0$ – the same temperatures as the weak coupling results shown in Fig.3 of the main text. The dashed line in panel (a) marks the "bare" resonance condition $\omega_1 = \omega_0 - \Omega$. Bottom: (c) engine average power in units of γ_2^2 and (d) efficiency normalized to the Carnot limit η_C as a function of κ and Ω for $\omega_1 = 0.4\omega_0$ and the same temperatures as above. The dashed line in panel (c) follows the resonance detuning of Eq. (117) – see text – the blue dot maps equivalent parameters. Other parameters are $\gamma_1 = \gamma_2 = 0.02\omega_0$.

response function $\chi(\omega)$ of the QHO, given in Eq. (15)). The coupling to the environment is responsible both of a damping of the QHO and of a shift of its energy, reflected by the poles of $\chi(\omega)$. Studying in particular the energy shift we find a renormalized frequency for the QHO, "dressed" with terms stemming from the coupling to the two environments. To a leading order, the dressed oscillator frequency can be found numerically solving the equation

$$\omega^2 - \omega_0^2 - \text{Re} \left[\tilde{k}_0(\omega) \right] = 0, \quad (116)$$

looking for a solution $\bar{\omega}_0(\kappa, \Omega)$ with the property $\bar{\omega}_0(\kappa, \Omega) \rightarrow \omega_0$ for $\kappa \rightarrow 0$. To obtain the detuned resonant drive frequency $\bar{\Omega}$ one can simply replace the bare oscillator frequency in the "bare" resonance equation and solve for $\bar{\Omega}$:

$$\omega_1 = \bar{\omega}_0(\kappa, \bar{\Omega}) + \bar{\Omega} \text{Sgn}(T_1 - T_2). \quad (117)$$

A plot of such $\bar{\Omega}$ is shown as a dashed line in Fig. 7(c). The agreement with the full numerical solution is excellent.